June 25, 2020

Responses to Reviewer #1

Thank you for your review of our paper: ESSD-2019-252. Below we paraphrase your comments in bold and provide our responses in regular text. We also recognize the challenging context of the COVID-19 pandemic as well, and are most appreciative of your review.

Needs substantial revision before acceptable to ESSD.
Data access comments, related to difficulty downloading the data from the Dryad repository, including suggestions to provide a "teaser data product" and a more prompt delivery of data.
We became aware of these issues when a few scientists contacted us about the data repository. We found that Dryad does in fact respond promptly, but because of the large file size sends an email with a URL for users to download the data. We have discovered that this email, unfortunately, is frequently filtered into the Spam folder. We added a note in the data description portion of the Dryad repository material to alert users to this situation. We note that the Dryad repository meets the requirements specified by ESSD. Part of the challenge is simply due to the fine-resolution global datasets and floating-point values that do not compress well. Also, while we recognize it isn't a permanent solution, we provided a URL: (https://davidtheobald8.users.earthengine.app/view/global-human-modification-change) for a dynamic mapping website that allows rapid visualization of our data, and comparison to a few other commonly referenced datasets.

I am worried about source data availability, particularly in relation to the use of Google Earth Engine.
You are correct that we did implement our analysis in Google Earth Engine (GEE) and did upload source data into the GEE platform to conduct our analysis. But, all source data used are open source and are accessible externally via the permanent DOIs that we provided. Furthermore, the formulas are carefully and clearly described, following the guidelines of ESSD in providing DOI permanent links to all source data and "recipe" used in the analysis to create the data product presented in the paper. Please note that we placed citations with DOI into the References section to streamline and make a more concise document by providing acronyms in Table 1.

Manuscript fails to present comprehensive estimates of uncertainty.
Thank you for your detailed comments on this important issue. In our response we address four aspects from the issue you raised regarding "uncertainty": (1) our ability to capture dynamic events, such as wildfire or climate change; (2) understanding the uncertainty of our results related to measurement error; (3) the precision with which we report results; and (4) including uncertainty in our validation analysis. We address each of these in order:

1. Uncertainties associated with dynamic events, land uses, and activities that we did not attempt to capture. We address this briefly in the caveat section and by citing our previous

work where we discuss these challenges, particularly around wildlife and climate change. We revised our text in the caveat section to read, on lines 563-573:

> *"As with any model, we recognize there are limitations of our work. We did not include data for all human stressors, largely because of incomplete global coverage or coarse mapping units (Klein Goldewijk et al. 2007; Geldmann et al., 2014), an inability to discern human-induced versus natural disturbances, or uncertainty in the location and directionality of its impact (e.g.; climate change on terrestrial systems; Geldmann et al., 2014). In particular and discussed in Kennedy et al. (2019a, 2019b), changes to land cover due to ecological disturbance events, such as wildfires or flooding, are not included in our analysis because of the difficulty in separating natural from human-caused disturbances -- yet, we recognize that the broad extent of wildfire in particular, could have strong implications. We did not include climate data as a stressor in this product to keep our analysis manageable and tractable. For more integrated analyses, our data product should be used in combination with datasets of impacts due to climate change (e.g., Parks et al. 2020)."*

2. We revised our manuscript to improve how we address how uncertainty affects our results for 2017 by conducting an additional analysis of the per-pixel variability (standard deviation) and adding Figure 4 which provides a map as well as summary results, providing values across the randomized iterations of the mode.
   Additionally, we realize that a few of the uncertainty measures we incorporated were dispersed in the methodology section when describing the modeling approach. We therefore added text in the revised Uncertainty and validation analysis section (quoted below in italics) to reiterate key aspects of the methodology that directly include uncertainty in the formulas used to calculate the human modification for each stressor. In particular we: (a) used the results from the accuracy assessment of the land cover dataset, to adjust weights associated with land cover types when estimating the degree of human modification (H); (b) similarly, we weighted our estimates for the urban/built-up stressor when calculating H, as a function of the degree of confidence of the modeled estimates provided by the GHSL dataset, on a per-pixel basis; and (c) addressed the spatial uncertainty associated with stressors represented as points (e.g., mine locations, gas flares) and lines (i.e. roads) when calculating H.
   The above mentioned revisions are included in Figure 4 and the revised text on lines 506-515:

   > *"We addressed uncertainty in our results by incorporating the parameter $p(C_s)$ for every sector s to best quantify uncertainty in its spatial location and classification as detailed in section 2.2.; for example, we adjusted $p(C_{cp})$ by directly incorporating measured confusion among land cover types using the results from the accuracy assessment of the land cover dataset (from Eq. 4). Additionally, we incorporated uncertainty by calculating the global mean for each of the 50 randomizations, which across the 50 iterations was 0.1434 (SD= ±0.0076) and ranged from 0.1243 to 0.1612. Thus, the global mean of 0.1461 obtained using our "best-estimate" intensity values was in line with our uncertainty results. We also mapped the per-pixel variance (standard deviation) to*

examine the spatial pattern of uncertainty (Figure 4). The locations of the highest levels of uncertainty tend to be in more highly developed landscapes."

3. We responded to your comment about our reporting of results without providing variance measures and overly-high precision by modifying our text to include a measure of human modification (which ranges from 0.0 to 1.0) using 4 orders of precision (i.e., +/- 0.0001 rather than +/- 0.00001) to be consistent with reporting percentages. As suggested, we also added a +/- when reporting our estimates of human modification in terms of area (i.e. square kilometers). This includes removing our statement that you found troubling regarding the 100 km^2 unit of analysis area. Changes occur on lines 28, 422, 435, 451-463, 511-12, and Tables 4-6.

4. We addressed your comment about validation: "Neither do the authors assign any uncertainty to so-called validation products HF or THPI", by clarifying the purpose of our validation analysis and how we accomplished it. We revised our manuscript text to clarify our steps, and included further citations that provide additional details. To be clear, we did not validate our results against the modeled outputs from the human footprint (HF) or human pressure index (THPI), rather, we simply *compared* our data to them because they are typically perceived as being similar, are readily-available and frequently used datasets, and we anticipated such a comparison will be a common and reasonable question of readers and data users. In fact, a central reason we have produced the work in this manuscript is to build on and provide a more refined and improved way to spatially represent and measure the degree of human modification on landscapes. That said, while we compared our data to other available products, we note that we did indeed validate our data by calculating and reporting the coefficient of determination (i.e. r^2) against "ground truth" data described in Kennedy et al. (2019a, 2019b) i.e., "our validation data" mentioned in lines 517-523:
   "We found strong agreement between H for ~2017 and our validation data (r=0.783), with an average root-mean-square-error of 0.22 and a mean-absolute-error of 0.04, for the 926 ~1 km^2 plots (9,260 sub-plots). There were 726 plots within ±20% agreement, while for 161 plots H was estimated higher than our visual estimate from the validation data (and 39 plots lower). Estimates of H were biased high, likely because the stressors for the "human intrusion" and electrical infrastructure (based on nighttime lights) are not readily observable from the aerial imagery used to generate the validation data. Our results here are consistent with our earlier findings (Kennedy et al. 2019a, 2019b, 2019c)."

Specific comments and suggestions below:
Page 2, lines 23-24, question about the duration of a breath:
Thank you -- following your questions and Reviewer #2's suggestion, we removed this "real-world" comparison from the manuscript.

Page 3, Line 49: Have [we] dismissed too many prior studies or contemporary work on human impact issues?

Thank you -- at your suggestion, we cited a few additional important works in the field, in particular the work on HYDE 3.2 product (https://doi.org/10.5194/essd-9-927-2017), Ellis' work on mapping the Anthromes, and recent work (Riggio et al. 2020) that compares human modification (Kennedy et al. 2019a), Human Footprint, Anthromes, as well as Jacobsen's (Jacobsen et al. 2019) and Riggio's work (Riggio et al. 2020). It is always a challenge to balance providing enough context for when developing new science. We chose to provide a more focused, technical description as the purpose of our paper is to develop a specific data resource that examines recent change (1990-2015) and relatively high-resolution for global work (0.3 km) -- rather than a broader review of similar previous efforts.

Page 3, line 60: Clarify wording: "...obstructions by vegetation canopy (e.g., some roads, trails)".
Good suggestion, we modified lines 59-62 to read:

> *"This is because remotely sensed imagery has limitations for this application -- especially prior to ~2010 -- because it can require human-interpretation to classify adequately and can miss development features that are obstructed by vegetation canopy or are small or narrow features (e.g., towers, wind turbines, powerlines)."*

Page 3, Line 69: clarify explanation of "...additive but monotonic relationships…"
Thanks, we simplified this sentence to clarify it on line 70, to read: "...measure that assumes additive relationships among stressors..."

Page 8, line 264: be consistent when listing metals with common names.
Thanks, we modified our text on line 266 to state "uranium oxide".

Page 10, line 337: Clarify why wildfires, if excluded in the analysis, do not show up as an uncertainty.
Good point, we added text to describe how wildfire (and other dynamic ecological processes) are considered within our work on lines 339-342:

> *"(Note that we excluded wildfire as a stressor because of the challenges of attributing wildfires to human causation-- especially over global extent, and urbanization because it is measured directly by the built-up stressor)."*

and lines 567-573:

> *"In particular and discussed in Kennedy et al. (2019a, 2019b), changes to land cover due to ecological disturbance events, such as wildfires or flooding, are not included in our analysis because of the difficulty in separating natural from human-caused disturbances -- yet, we recognize that the broad extent of wildfire in particular, could have strong implications. We did not include climate data as a stressor in this product to keep our analysis manageable and tractable. For more integrated analyses, our data product should be used in combination with datasets of impacts due to climate change (e.g., Parks et al. 2020)."*

Page 12, line 418: clarify and be consistent with area estimate, and remove reference to football pitches.
Thanks, done.

Page 12, lines 423-4. Clarify why available climate change datasets are not used.
Thanks, this is an important point. We agree that climate change effects are happening, and there are numerous climate data products and a burgeoning field of science. To address this point, we clarified our decision not to include it in our analysis on lines 116-123:

> *"To estimate the current amount of H circa 2017 year (median=2017, min=2012, max=2019), we included three additional stressors, including grazing, oil and gas wells, and powerlines. We note that we did not map stressors for invasive species or pathogens and genes, geologic events, or climate change. This was because suitable temporal global data were not available to capture stressors due to invasive species or pathogens and genes; the majority of geological events are not directly caused by humans; and climate change is better modeled as separate process distinct from the effects of direct human activities and has a plethora of research on this topic (Geldmann et al. 2014; Titeux et al. 2016)."*

and on lines 571-573:

> *"We did not include climate data as a stressor in this product to keep our analysis manageable and tractable. For more integrated analyses, our data product should be used in combination with datasets of impacts due to climate change (e.g., Parks et al. 2020)."*

Sincerely,

David M. Theobald, Ph.D., on behalf of co-authors

June 25, 2020

Reviewer #2

Thank you for your review of our paper: ESSD-2019-252. Below we paraphrase your comments in bold (for clarity), and provide our responses in regular text. We also recognize the challenging context of the COVID-19 pandemic as well, and are most appreciative of your review.

This new dataset represents an important advancement in our assessment of natural areas and human impacts… Thank you for this contribution.
Thanks!

My only concern is how water is dealt with, that for some uses such as modeling ecological processes or species movement it would be valuable to at least produce a version of the dataset that has all water bodies masked out.
This is an important comment, and we appreciate your suggestion to provide a second version of the data with water bodies removed. We believe including reservoirs to include the modification of ecological processes through habitat loss and fragmentation of the artificial water bodies is an important advance. Yet, we recognize there can be situations where removing all waterbodies may be more suitable for a given problem. To address this, we also added a separate land/water mask dataset to the repository to allow users to readily remove reservoirs so as to treat all waterbodies in a similar fashion. We updated the manuscript to note this addition in the Data Availability section.

A minor point -- revise the sentence containing: "...over the pause of a deep breath".
Thank you -- we have revised to read more simply: "... over 12 hectares each minute."

Sincerely,

David M. Theobald, Ph.D., on behalf of co-authors

June 25, 2020

Responses to Reviewer #3

Thank you for your review of our paper: ESSD-2019-252. Below we paraphrase your comments in bold and provide our responses in regular text. We also recognize the challenging context of the COVID-19 pandemic, and are most appreciative of your review.

General comments: The presented dataset can be highly valuable for both research and decision making. However, some clarifications and revisions are needed beside the concerns already raised by Reviewer 1 and 2. Most importantly, I recommend the authors to share the complete dataset and clearly describe the dataset provided.
Thank you. To address your general comment, we have revised our dataset repository (DOI) to clarify and provide additional details on major stressor types to document file naming and structure. In addition, we respond to specific comments that are related to this general one below.

Provide datasets for the individual stressors that comprise the overall human modification dataset
We grouped individual stressors into major categories: urban/built-up, agriculture, energy/mining, and transportation/service, and all individual stressor data are readily available and/or are fully documented in our paper. Providing a copy of those data in our repository is somewhat redundant and unfortunately in some cases, would verge on license issues.

Data repository: It would be useful if the authors could provide a readme file (or improve the usage note description on Dryad) for the data provided, perhaps a table listing what files and data are actually shared. (I only tried to check on the data using Python, not sure if use of e.g., Google Earth Engine would have shown anything differently. If there are differences, the authors could perhaps try to bridge the differences or recommend a preferred software.)
Thank you for this suggestion. We have improved the usage note description associated with the Dryad repository (please refer to the revised text from that document above). We note here that there is no additional meta-data content provided in the Google Earth Engine view of these data.

What do the folder names represent (e.g. "60c vs. 60s")? What files are associated with each folder?
We have simplified the datafile and folder structure, and described this structure fully in the data description of the repository, to the following. When unzipped, each zip file expands to a folder with the constituent files:
gHMv1_300m_1990_change.zip
gHMv1_300m_2000_change.zip
gHMv1_300m_2010_change.zip
gHMv1_300m_2015_change.zip
gHMv1_300m_2017_static.zip
gHMv1_300m_2017_static_stressors.zip

gHM_landLakeReservoirOcean300m.zip

Regarding potential error on file gHMv1_1990_1000_60c_land-0000000000-0000000000…
We confirmed that all source data are correct by downloading data from the repository and recreating our datasets from the repo. Perhaps your error was related to a download error? Regardless, we tested the viability of our data posted on Dryad by downloading and displaying data.

Manuscript mentions 2017 dataset but no folders contain 2017?
As described above, we changed the naming conventions to be clearer, including distinguishing 2017 data.

Global datasets for 1990, 2000, 2010, and 2015… but where are the 2000 and 2010 data?
As described above, we changed the naming conventions and explicitly provided the 2000 and 2010 data.

Suggestion to complement the lat/lon/date and unit info in embedded metadata?
We added this information to the data description.

Data description mentions change stressors and uncertainty analyses, are these included in Dryad?
Good suggestion. We added to the data repository 4 additional datasets that provide stressors.

Manuscript comments
Consider adding a time index in the stressor equations for the variables that vary in stressor equations to make temporal variables more explicit.
Thank you for this suggestion. We addressed this suggestion by including this information into Table 1 (see response to comment directly below) because we felt it was more explicit as to the time-varying stressor datasets.

Table 1. Clarify stressors that are used for 1990-2015 and the 2017 datasets.
Thanks -- we added year columns to Table 1 to clarify the specific years of data for each stressor and to distinguish the "change" datasets from the static dataset (representing "current" ~2017 conditions.)

To facilitate interpretation of comparison results, It might be useful to provide an overview table or description of how datasets and/or methodology different between human footprint, temporal human pressure index, and human modification.
This is a valuable suggestion -- we added a new table (Table 6) that describes the differences in datasets and/or methodology between our work here and other recent datasets.

Consider changing "Hmed" to "Hmedian" to ease reading and confusion with other variables.
Thanks, done.

L433: Comment on the differences between the bottom line findings as compared to Ramunkutty et al. and FAO findings. Why do they differ so much?
Good suggestion. We added a discussion of the differences with Ramunkutty et al. as detailed in our response to L476 below but elected to not cite FAO findings because those data are conducted using very different methods and scales -- though their estimates are also based on land cover and do not include intensity (further response in comment below).

L476: Comment on the differences of your findings with HF and Hurtt et al. 2006 finding.
Following the above comment on L433, we briefly describe the differences in our finding with HF and Ramunkutty et al. (2008). We chose to not cite Hurtt et al. (2006), as they provide summary findings largely based on Ramunkutty et al. (2008). We revised our text to read (L483-496):

> *"The biggest differences in rankings between the H and the HF were for temperate and broadleaf mixed forests (and see comparisons of H1k and HF in Kennedy et al. 2019a, 2019b, Riggio et al. 2020). HF was estimated to result in 12.3% modification for an earlier date (~2009; Venter et al. 2016) and is lower likely because fewer stressors were included, its additive combination method, and its strongly right-skewed distribution caused by max-value normalization. The ranks of the extent of modification by biomes, however, were very similar between H, H1k, and HF. In general, H had intermediate modification levels compared to H1k and HF: with H1k levels being slightly higher (difference between 0.00 min to 0.09 and average difference of 0.05 by biome) and HF being slightly lower (difference between 0.00 min to 0.13 max and average difference of 0.04 by biome; Table 7). Results for ecoregions shown in Fig. 1 are even more striking, as the mean annualized difference values for HF and THPI were inconsistent with our results. Of the 814 ecoregions that had increases in H_{mad}, a decrease in modification was found for 201 ecoregions in HF_{mad} and 202 for $THPI_{mad}$; and for the 32 ecoregions that were found to have decreases in H_{mad}, an increase in modification was found for 20 in HF and 22 in THPI."*

Related to Reviewer #1's comment, consider for increased usability providing an "overview" a 0.5 degree resolution dataset.
Thank you for this suggestion. While we understand these files can take long to download depending on internet access, we opted to maintain the original resolution, anticipating (from experience), that having multiple versions will lead to confusion and likely different (albeit slightly) results due to resolution differences. In this way, potential users can aggregate this dataset into multiple scales based on their specific purpose. To address the need for reduced download file size, we changed the datasets from 32-bit floating point to a 16-bit integer, which reduces each dataset by half or more (with LZW compression).

Sincerely,

David M. Theobald, Ph.D., on behalf of co-authors

Earth transformed: detailed mapping of global human modification from 1990 to 2017

David M. Theobald[1,2], Christina Kennedy[3], Bin Chen[4], James Oakleaf[3], Sharon Baruch-Mordo[3], Joe Kiesecker[3]

[1]Conservation Planning Technologies, Fort Collins, CO 80521, USA

[2]Department of Fish, Wildlife, and Conservation Biology, Colorado State University, Fort Collins, CO 80523, USA

[3]Global Lands Program, The Nature Conservancy, Fort Collins, CO 80524, USA

[4]Department of Land, Air and Water Resources, University of California, Davis, CA 95616, USA

Correspondence to: David M. Theobald, Ph.D. (dmt@davidmtheobald.com)

Abstract

Data on the extent, patterns, and trends of human land use are critically important to support global and national priorities for conservation and sustainable development. To inform these issues, we created a series of detailed global datasets for 1990, 2000, 2010, and 2015 to evaluate temporal and spatial trends of land use modification of terrestrial lands (excluding Antarctica). We found that the expansion and increase of human modification between 1990 and 2015 resulted in 1.6 M km^2 of natural land lost. The percent change between 1990 and 2015 was 15.2% or ~~0.61~~0.6% annually -- ~~roughly 177~~about 178 km^2 daily~~. Over the pause of a deep breath, over 8 football pitches of natural lands were lost (~17 per~~, or over 12 hectares each minute~~)~~. Worrisomely, we found that the global rate of loss has increased over the past 25 years. The greatest loss of natural lands from 1990-2015 occurred in Oceania, Asia, and Europe, and the biomes with the greatest loss were mangroves, tropical & subtropical moist broadleaf forests, and tropical & subtropical dry broadleaf forests. We also created a contemporary (~2017) estimate of human modification that included additional stressors and found that globally ~~14.5~~14.6% or 18.5 M km^2 (±0.0013) of lands have been ~~completely~~ modified -- an area greater than Russia. Our novel datasets are detailed (0.09 km^2 resolution), temporal (1990-2015), recent (~2017), comprehensive (11 change stressors, 14 current), robust (using an established framework and incorporating classification errors and parameter uncertainty), and strongly validated. We believe these datasets ~~will support better~~support an improved understanding of the profound transformation wrought by human activities and provide foundational data on the amounts, patterns, and rates of landscape change to inform planning and decision making for environmental mitigation, protection, ~~restoration, and adaptation to climate change~~and restoration. The datasets generated from this work are available ~~here (Figshare DOI pending~~at https://doi.org/10.5061/dryad.n5tb2rbs1 (Theobald et al. 2020).

1 Introduction

Humans have transformed the earth in profound ways (Marsh 1885; Jordan et al. 1990; Vitousek et al. 1997), contributing to global climate change (IPCC 2019), causing global habitat loss and fragmentation, and contributing to declines in biodiversity and critical ecosystem services (IPBES 2019). Addressing the consequences of rapid habitat loss and land use change are essential for implementation of various international initiatives, including the Convention on Biological Diversity 2020 Aichi Biodiversity targets, the United Nations 2030 Sustainable Development Goals (esp. Goal 15; Secretariat of the Convention on Biological Diversity, 2010), the Bonn Challenge (Verdone & Seidl, 2017), and the Global Deal for Nature (Dinerstein et al. 2019). Foundational to addressing these goals is a firm understanding of the rates, trends, and amount of these land use changes. Efforts to date have focused on historical patterns (Klein Goldewijk et al. 2007~~; Venter et al. 2016; Geldman et al. 2019; Kennedy et al. 2019a) have been limited due to the unavailability of contemporary, temporally comparable, and high-resolution data~~, 2017; Ramankutty et al. 2008; Ellis 2018) or have been limited due to the unavailability of contemporary, temporally comparable, and high-resolution (< 1 km^2) data (Venter et al. 2016; Geldman et al. 2019; Kennedy et al. 2019a).

Here we describe a new dataset ~~to estimate the human modification (HM)~~that maps the degree of human modification of terrestrial ecosystems globally, for recent changes from 1990 to 2015, and for contemporary (circa 2017) conditions. We mapped human activities that directly or indirectly alter natural systems, which we call anthropogenic drivers of ecological stress or "stressors" (following Salafsky *et al.*, 2008; Theobald 2013). Similar to other efforts (Sanderson et al. 2002; Theobald 2010, 2013; Geldmann et al. 2014; Venter et al. 2016; Kennedy et al. 2019a), we augmented remotely-sensed data with traditionally-mapped cartographic features. This is because remotely sensed imagery has limitations for this application -- especially prior to ~2010 -- ~~including obstructions by vegetation canopy (e.g., some roads, trails), inability to detect small or narrow features (e.g., towers, wind turbines, powerlines), or can require human-interpretation to classify efficiently.~~~~¶~~

¶

~~We quantified HM~~because it can require human-interpretation to classify adequately and can miss development features that are obstructed by vegetation canopy or are small or narrow features (e.g., towers, wind turbines, powerlines).

We mapped the degree of human modification based on an established approach that has been applied nationally, internationally, and globally (Theobald 2010, 2013; Gonzalez-Abraham et al. 2015; Kennedy et al. 2019a). It uses an existing classification system (Salafsky *et al.*, 2008) to: (a) ensure parsimony; (b) distinguish two spatial components (area of use and intensity of use); (c) use a physically-based measure that is needed to estimate change (Gardner and Urban 2007); (d) incorporate spatial and classification uncertainty; and (e) combine multiple stressors into an overall measure that assumes additive ~~but monotonic relationships~~relationships among stressors and addresses the correlation among variables (Theobald 2010). The resulting ~~estimate is a quantitative measure of HM with~~quantitative estimate of human modification has values ranging from 0 to 1 that support robust landscape assessments (Schultz 2001; Hajkowicz and Collins 2007).

To understand temporal landscape change, we calculated ~~*H*~~the degree of human modification -- denoted by *H* -- for the years 1990, 2000, 2010, and 2015 using methods and datasets that minimize noise and bias. Second, we included additional stressors not incorporated previously, including disturbance of natural processes due to reservoirs, effects from air pollution, and human intrusion (Theobald 2008). Third, we calculated human stressors using up to two orders of magnitude finer resolution data (0.09 vs. 1-86 km^2) than past efforts (Ellis and Ramankutty 2008; Geldmann et al. 2014; Haddad et al. 2015; Venter et al. 2016; Geldmann et al. 2019b; Kennedy et al. 2019a). This higher resolution reduces the loss of information of the spatial pattern within a pixel, better identifies rare features, facilitates the application of these data for species and ecological processes that often occur at a fine-scale, and improves the utility and relevance of these products for policy makers, decision makers, and land use managers.

Calculating *H* as a real value across the full gradient of landscape ~~changes~~change is valuable because it can be applied rigorously to a variety of questions (Theobald 2010, 2013), including discerning the heterogeneity of human uses that are often lumped within broad classes like “urban”~~,~~; capturing the extent and pattern of the agricultural lands typically occurring beyond urban centers and protected areas~~,~~; and delineating areas of low modification~~—~~: all of which are useful for conservation prioritization and planning efforts (Kennedy et al. 2019a, 2019b). Here, we describe the technical methods and briefly report on results on the temporal trends and current spatial patterns of human modification across all terrestrial lands, continents, biomes and ecoregions ~~(Dinerstein et al. 2017)~~. Because conservation organizations often use this type of data to focus their activities on specific regions (e.g., Jantke et al. 2019), we provide rankings by biome and ecoregion (Dinerstein et al. 2017) and briefly compare our results to other available ~~results~~studies.

2 Methods

2.1 Overview

We calculated the degree of human modification using the Direct Threats Classification v2 (Salafsky et al. 2008; cmp-openstandards.org), which defines a stressor as the proximate human activities or processes that have caused, are causing, or may cause impacts on biodiversity and ecosystems. Table 1 lists the specific stressors and data sources we included in our maps: urban/built-up, crop and pasture lands, livestock grazing, oil and gas production, mining and quarrying, power generation (renewable and non-renewable), roads, railways, power lines and towers, logging and wood harvesting, human intrusion, reservoirs, and air pollution.

To estimate *temporal change* in ~~HM~~*H* from 1990 to 2015, we followed ~~criteria established~~established criteria (Geldmann et al. 2014) and included 11 stressors for which we could obtain global data with fine-grained resolution (~~<~~≤1 km^2), and that provided consistent and comparable repeated measurements, especially in regards to the data source, methods used, and appropriate time frame (Table 1). We included current major roads and railways as a static layer in the temporal maps because in most cases some form of road existed prior to our baseline year of 1990 (except for the relatively rare, though important, new highway constructed).

To estimate the *current* amount of ~~HM~~*H* circa 2017 year (median=2017, min=2012, max=2019), we included three additional stressors, including grazing, oil and gas wells, and powerlines. We note that we ~~were~~did not ~~able to~~ map stressors for invasive species or pathogens and genes, geologic events, or climate change. This was because suitable temporal global data were not available to capture stressors due to invasive species or pathogens and genes; the majority of geological events are not directly caused by humans; and climate change is better modeled as separate process distinct from the effects of direct human activities and has a plethora of research on this topic (Geldmann et al. 2014; Titeux et al. 2016).

For each stressor *s* we quantified ~~HM (denoted by *H*) using~~the degree of human modification as:

$$H_s = F_s * p(C_s) * I_s , \tag{1}$$

where ~~F~~F_s is the proportion of a pixel occupied (i.e. the footprint) by stressor *s*, $p(C_s)$ is the probability that a stressor occurs at a location to account for spatial and classification uncertainty, and ~~I~~I_s is the intensity. Importantly, *F* and *I* have a direct physical interpretation (Gardner and Urban 2007), are well-bounded and range from 0-1, and values are a “real” data-type. Consequently, *H* provides the basis for unambiguous interpretation to assess landscape change (Hajkowicz and Collins 2007; Riitters et al. 2009). Specific formulas used to map raw stressor data as indicator layers are provided below. Table 2 details our estimates of intensity values for each stressor (modified from Theobald 2013 and Kennedy et al. 2019a), which is used to differentiate land uses that have varying impacts on terrestrial systems (e.g., grazing is less intensive than mining). Our intensity values were informed by standardized measures of the amount of non-renewable energy required to maintain human activities (Brown and Vivas 2005) and found to generally correlate with species responses to land use where examined (Kennedy et al. 2019a).

We generated datasets that represent temporal changes between 1990 and 2015 and for current (~2017) conditions by combining stressor layers using the fuzzy algebraic sum (Bonham-Carter, 1994; Malczewski 1999; Theobald 2013), which is calculated as:

$$H = 1 - \prod_{s=1}^{n} (1 - H_s) , \tag{2}$$

where *n* is the number of stressors (*s*) included. Of critical importance, the fuzzy sum formula is an *increasive* function that calculates the cumulative effects of multiple stressors in a way that minimizes the bias associated with non-independent stressors and assumes that multiple stressors accumulate (Theobald 2010, 2013; Kennedy et al. 2019a). This differs substantially from simple additive calculations that are commonly used (Halpern et al. 2008; Halpern and Fujita 2013; Venter et al. 2016), but assume that stressors are independent and results in a metric that is sensitive to the number of stressors included in the model (Malczewski 1999).

We mapped human modification of all terrestrial lands (excluding Antarctica) and included lands inundated by reservoirs, but excluded other rivers and lakes. An often overlooked but critical aspect to understand human modification is how water is mapped, especially for the interface between land

and coastlines, lakes, reservoirs, and large rivers. We mapped non-reservoir areas dominated by water (i.e., oceans, lakes, reservoirs, and rivers) by processing data on ocean from the European Space Agency's Climate Change Initiative program (ESA CCI; ~~150 m~~0.15 km, circa 2000) and surface waters using the Global Surface Water dataset (GSW; 30 m; Pekel et al. 2016). We identified inland water bodies (i.e. lakes, reservoirs, rivers, etc.) using ESA CCI non-ocean pixels that were at least 1 km from the interior of the land-ocean interface. We identified interior water pixels using GSW with at least 75% water occurrence from 1984-2019 and that were at least 0.0225 km^2 in area (to remove small lakes, ponds, and narrow streams). As a result, inland water bodies and the ocean-land interface are ~~much clearer~~more distinct , more consistent, and better aligned.

We summarized our estimates of human modification ~~(H)~~ across all terrestrial lands, biomes, and ecoregions (defined by Dinerstein et al. 2017) and here report median (~~H_{med}~~H_{median}) and mean (H_{mean}) statistics. We summarized results of temporal trends using the mean annualized difference (H_{mad}), calculated as the mean ~~value~~values across each analytical unit (e.g., biomes, ecoregions) of the annualized difference assuming a linear trend (H_{ad}):

$$H_{ad} = (H_u - H_t)/(u - t) , \quad (3)$$

where *u* and *t* are the years of the datasets (e.g., u=2015, t=1990) and $u > t$. When discussing trends between 1990 and 2015, we emphasize the mean statistic because it better captures locations where *H* values have changed (mostly increasing over time), partly due to land uses with high values (e.g., urbanization ~0.8) that are not well represented in the median statistic. We calculated the increase in ~~HM~~H, or conversely the amount of natural habitat loss, as the per-pixel ~~H~~ value times the pixel area, summed across a given unit of analysis. This assumes that any increase in the level of human modification causes natural land loss regardless of the original *H* level. We also report the median statistic because, as is typical of spatial landscape data, the distribution of *H* values is skewed to the right. Finally, we compared our results of H_{mad} to those calculated on the Human Footprint (HF for 1993-2009; Venter et al. 2016) and the temporal human pressure index (THPI for 1995-2010; Geldmann et al. 2019b).

2.2 Stressors mapped

2.2.1 Urban and built-up

To map built-up areas that are typically found in urban areas and dominated by residential, commercial, and industrial land uses, we used the most recent version of the Built-up Grid from the Global Human Settlements Layers dataset (GHSL R2018A; Pesaresi et al. 2015). The degree of ~~HM~~human modification that is contributed by built-up areas, H_{bu}, is:

$$H_{bu} = F_{bu} * p(C_{bu}) * I_{bu} , \quad (4)$$

where F_{bu} measures the proportion of the area of a pixel classified as built-up, $p(C_{bu})$ applies the GHSL-reported confidence mask (for 2014) for locations of the built-up areas (for the target year; Pesaresi et al. 2015) and I_{bu} is the intensity factor specified in Table 2.

2.2.2 *Agriculture*

We mapped agriculture stressors by identifying land cover classes associated with crop and pastureland from ESA CCI land cover datasets (ESA CCI 2015; Perez-Hoyos et al. 2017; Li et al. 2018) available at 0.09 km^2 for 1992, 2000, 2010, and 2015. We merged the cropland and pastureland stressors because these two classes are combined in the ESA land cover data, and they are challenging to distinguish even at higher resolution (~30 m, Wickham et al. 2017). To incorporate classification errors associated with all cover classes, we multiplied the footprint F_{cp}= 1.0 times the probability ~~$p(C_{cp})$~~ that a pixel with cover class C was found to be cropland or pasture, ~~C_{cp}~~ $p(C_{cp})$, by interpreting reported accuracy assessment results (ESA CCI 2017, in Table 3). To reduce the effects of scattered pixels that have some probability of being mapped as cropland-pastureland (e.g., misclassified pixels high-elevation tundra or alpine areas), we multiplied $p(C_{cp})$ by the proportion of lands estimated to be in crops from the Unified Cropland Layer (Waldner et al. 2016), *v* so that:

$$p(C_{cp})' = p(C_{cp}) \times v \quad , \qquad (5)$$

and also reduced the value of $p(C_{cp})'$ based on patch size *A*, assuming that accuracy declines rapidly with cropland/pastureland small "patches" (A < 1 km^2) using:

$$p(C_{cp})'' = (p(C_{cp})')^2 \quad , A < 1 . \qquad (6)$$

We then calculated H_{cp} as:

$$H_{cp} = F_{cp} * p(C_{cp})'' * I_{cp} . \qquad (7)$$

We developed spatially-explicit estimates of agricultural intensity based on land management, such as cropping and number of rotations, tilling, and cutting operations, because these activities typically vary geographically (van asselen and Verburg 2012; Kehoe et al. 2017). We followed existing methods (Chaudhary and Brooks 2018) to estimate three intensities of agricultural land use -- minimal, light, and intense -- and then mapped them using cover types from Global Land Systems v2 dataset (GLS; Kehoe et al. 2017) by estimating intensity values (*I*) for each of the agricultural intensity types (Table 2). Although GLS v2 represents conditions circa 2005, we incorporated temporal changes by weighting the ~~proportion~~proportions of agricultural lands from the time-varying ESA CCI land cover datasets.

To estimate the modification associated with the grazing of domestic livestock (H_{au}), we used the Gridded Livestock of the World v3 (Robinson et al. 2014; Gilbert et al. ~~2018~~2018a, Gilbert et al. 2018b) that maps the density of animals per km^2 (G) for eight types of livestock (*j*): buffaloes, cattle, chickens, ducks, goats, horses, pigs, and sheep. To calculate the overall footprint of grazing (F_{au}), we summed the weighted densities by global averages of livestock unit (*LU*) coefficients (w_i= 0.84, 0.67, 0.01, 0.01, 0.10, 0.84, 0.23, 0.10, listed respectively for each livestock species stated above). We used a lower threshold found at 10% to remove values <1.0 LUs/km^2 (similar to Jacobson et al. 2019) and 1000 *LU* km^{-2} as an upper threshold because it is a common breakpoint between grazing and industrial feedlots (Gerber et al. 2010). We assumed (here, and below unless otherwise provided) no uncertainty ($p(C_{au})$ = 1.0), because we lacked explicit data to do so. We then log_{10} transformed and max-normalized (Kennedy et al. 2019a) to obtain 0-1 values, and calculated the mean H_{au} using a 10 km radius moving window to reduce the effects of the coarser-resolution pixels:

$$F_{au} = \sum_{j=1}^{8} G_j w_j \text{, max(1000), min(1)} \tag{8}$$

$$H_{au} = ((log\,(F_{au} + 1))/\, log(1000) * \; p(C_{au}) * I_{au} \;\; . \tag{9}$$

2.2.3 Energy and extractive resources

To estimate stressors associated with extractive energy production, we mapped gas flares derived from "night-time lights" using data from the Visible Infrared Imaging Radiometer Suite from the Suomi National Polar-orbiting Partnership (VIIRS; Elvidge et al. 2013). Roughly 90% of gas flares occur at locations where oil and gas are extracted (Elvidge et al. 2015). We used point data processed specifically to identify gas flares in VIIRS for 2012/2013 (Elvidge et al. 2016). For each flare, we approximated a footprint of 0.057 km^2 per well head (Allred et al. 2015). It is common to approximate the footprint of points (and lines) using a simple "buffer", which implicitly assumes no location error and no distance-decay from the point of origin. Such a buffer approach essentially centers a cylinder on each data point, where volume (*V*) equals the approximate footprint and height (*h*) and a perfect certainty of 1.0. Here, however, we assumed some uncertainty in the location of the point and that the effects associated with a feature such as an oil/gas well-head diminish with distance. That is, rather than use a cylinder with volume *V* (or similarly a simple uniform buffer away from linear features, e.g. powerlines or roads), we used a conic shaped kernel centered on the point to calculate the uncertainty $p(C_{og})$, where the height of the cone *h*=0.5 represents a conservative estimate of spatial accuracy (Theobald 2013). We derived the cone radius *D* =0.329 km by setting *V* to the footprint of 0.057 km^2:

$$D = \sqrt{(3/h)\,V/\pi}\ , \tag{10}$$

Thereby the uncertainty parameter for each point is calculated using:

$$p(C_{og}) = 3h/\pi D^2\,. \tag{11}$$

We assigned the value of $p(C_{og})$ that overlapped the center of each pixel, with max $p(C_{og})$ = 1.0. Human modification was then calculated as:

$$H_{og} = F_{og} * p\,(C_{og}) * \; I_{og} \;\; . \tag{12}$$

2.2.5 Mines and quarries

To estimate modification due to mines and quarries, we derived locations represented as points from a global mining dataset (*n*=34,565; S&P 2018; Valenta et al. 2019). We retained surface mines that were constructed, construction started, in operation, in the process of being commissioned, or residual production (*n*=22,705). For the temporal change analysis, we removed locations that did not have a specified year of construction (*n*=3,634). We calculated the mean disturbed area and associated infrastructure of a mine by intersecting mine point locations with 441,623 polygons that represent footprints of quarries/mines (OpenStreetmap, 2016). For four types of mines: coal; hard-rock (bauxite, cobalt, copper, gold, iron ore, lead, manganese, molybdenum, nickel, phosphate, platinum, silver, tin, ~~U_3O_8~~uranium oxide, and zinc); diamonds; and other (antimony, chromite, graphite, ilmenite, lanthanides, lithium, niobium, palladium, tantalum, and tungsten), we estimated the mean area (*a*) to be: 12.95 km^2 (*n*=647) for coal, 8.54 km^2 (*n*=860) for hard-rock , 5.21 km^2 (*n*=39) for diamonds, and 3.40 km^2 (*n*=27) for other. Finally, following equations 8 and 9, we calculated $p(C_m)$

for each of the four mining types using D of 4.973, 4.038, 2.548, and 3.154 km, respectively, and calculated H_m as:

$$H_m = F_m * p(C_m) * I_m \ . \tag{13}$$

2.2.6 Power plants

To estimate the effects of where energy is produced, we mapped the location of power plants represented as points (n=29,903; WRI 2019). For the temporal change analysis, we removed locations that did not have a specified year of construction (n=16,288). We estimated $p(C_{pp})$ using a conic-shaped kernel (Eqs. 8 and 9) and h=0.5. We mapped both non-renewable energy forms (H_{ppn}; coal, oil, natural gas) and renewable energy forms (H_{ppr}; geothermal, hydro, solar, wind), where we assumed F_{pp}=1 and calculated a single $p(C_{pp})$ for both non-renewable and renewable energy sectors with D_{pp}=1224 m (following Theobald 2013):

$$H_{ppn} = F_{pp} * p(C_{ppn}) * I_{ppn} \ , \tag{14}$$

$$H_{ppr} = F_{pp} * p(C_{ppr}) * I_{ppr} \ . \tag{15}$$

2.2.7 Transportation and service corridors

For transportation, we mapped roads and railways using OpenStreetMap highway linear features (OpenStreetMap, 2019). We calculated the footprint for the following transportation types: major (motorway, primary, secondary, trunk, link), minor (residential, tertiary, tertiary-link), two-track roads and railways as:

$$F_{rr} = \sum_{i=0}^{c} (w / \alpha) * \mu \, , \tag{16}$$

$$H_{rr} = F_{rr} * p(C_{rr}) * I_{rr} \, , \tag{17}$$

where w is the estimated width of a road of type i from Table 2, α is the pixel width (i.e. 300 m), and μ=0.79 to adjust for the fractal dimension of road lines crossing cells (Theobald 2000) because road lines often cross pixels at random angles. If a divided highway is represented as two separate lines, then each is represented independently. Also, if a cell has two or more roadway types cross it (e.g., where a secondary road joins a highway), the fuzzy sum of H_{rr} for both roads is calculated. Note that *use* of roads is incorporated into the "human intrusion" stressor (described below).

To map the modification associated with above-ground powerlines (H_{pl}), we used:

$$H_{pl} = F_{pl} * p(C_{pl}) * I_{pl} \ , \tag{18}$$

where F_{pl} is calculated using a 500 m buffer (Theobald 2013), and $p(C_{pl})$ is calculated using h=0.5, and I_{pl} is the estimate of intensity.

To estimate a stressor associated with electrical infrastructure and energy use (H_{nl}), we mapped "night-time lights" using the Defense Meteorological Satellite Program/Operational Linescan System (DMSP/OLS; Elvidge *et al.*, 2001) "stable" lights dataset. We included this as a distinct stressor from the energy extraction stressor (oil and gas flares, discussed above) because gas flares are derived by finding anomalies (high values) in the images rather than from the "stable lights" product, and the footprints associated with the flares are an extremely small fraction of the overall extent of energy infrastructure.

To maximize temporal consistency, we used the intercalibrated DMSP/OLS dataset (Zhang et al. 2016; Li and Zhou 2017) and extended their approach for 2013 (using a=1.01 , b=0.00882, c=-0.965; Zhang et al. 2016). DMSP/OLS values, L, are expected to range from 0 to 63, but because max values differed yearly (ranging from 57.87 - 66.16), we normalized all images (1992-2013) to range from 0 to 1.0 using the max-adjusted value for each year (L'). To reduce the effects of noise in the images in areas with low-light and in high northerly latitudes, we removed nighttime light values when L'<0.077 -- that is, we set values to *null* when they were below the 25^{th} percentile of the global terrestrial distribution compared to the often used noise threshold of L=5 (following Elvidge et al. 2001).

To adjust for inter-annual spatial-misalignment errors (Elvidge et al. 2013), we adjusted the normalized DMSP image for 2013 to align with the 2013 VIIRS product by identifying sharply contrasting and consistent signals at 10 locations (n=10) distributed across the continents. We then visually compared each of the images from 1992-2012 to the DMSP image for 2013 and shifted the images to align them (averaged shift in meters: x=359.5, y=476.2). To further reduce inter-annual variability, we averaged image values at each pixel using a 3-year "tail" and used a rank-ordered-centroid weighting (Roszkowska 2013) such that the spatially-aligned and temporally-smoothed nightlight value Y for year t is:

$$Y_t = (L_t' * 0.62) + (L_{t-1}' * 0.26) + (L_{t-2}' * 0.12) \quad . \qquad (19)$$

Finally, to reduce the blooming effects and to take advantage of the higher-quality VIIRS-based nightlights (i.e. higher spatial resolution, reduction of saturated pixels), we sharpened DMSP nightlight values y_t using the VIIRS brightness value y to be proportional to the ratio of the DMSP values:

$$Y_t' = Y_t * (L_t' \div L_{2013}) \ . \qquad (20)$$

We then transformed Y_t' following Kennedy et al. (2019a), capping values above 126.0 (the 99.5 percentile of global values):

$$H_{nl} = (log_{10}(1 + Y_t') / 2.104)) * p(C_{nl}) * I_{nl} \ . \qquad (21)$$

2.2.8 Logging

To estimate stressors on forested lands, we used maps of forest loss (Curtis et al. 2018) associated with commodity-driven deforestation, shifting agriculture, and forestry. (Note that we excluded wildfire as a stressor because of the challenges of attributing wildfires to human causation-- especially over global extent, and urbanization because it is measured directly by the built-up stressor). We then identified locations where forest was lost due to one of the three mapped stressors (using v1.6, updated to 2018; Hansen et al. 2013) prior to the year of our estimated human modification map, and applied the intensity value associated with that stressor ~~(Table 2)~~. Thus,

$$H_{fr} = F_{fr} * p(C_{fr}) * I_{fr} \quad , \qquad (22)$$

where F_{fr} is pixels of forested loss in a given year, and I_{fr} is an estimate of intensity associated with the cause of forest loss.

2.2.9 Human intrusion

We estimated human intrusion ~~H_i~~ (H_i) using a method that builds on and extends accessibility modeling (Nelson 2008; Theobald 2008, 2013; Theobald et al. 2010; Weiss et al. 2018; Nelson et al. 2019). Human intrusion (aka "use": Theobald 2008) uses central place theory (Alonso 1960) and integrates human accessibility throughout a landscape from defined locations, typically along roads and rails as well as off-road areas from urban areas (Theobald et al. 2010; Esteves et al. 2011; Theobald 2013; Larson et al. 2018).

Accessibility measured in travel time in minutes is calculated from each mapped settlement point *j* (e.g., cities, towns, villages) from GRUMP v1.01 and GPW v4 (CIESIN 2017, 2018). This approach is much less sensitive to arbitrary thresholds of city/town size (e.g., 50,000 residents), often used due to computational constraints (e.g. Nelson 2008; Weiss et al. 2018). Second, to estimate "intrusion" of people to adjacent areas from a given settlement, we estimated the number of people (using population estimates at settlement *j*) at a given location (X; ~population density: people/km^2) following the assumption that the human density halved with every 60 minutes traveled (Theobald 2008, 2013). The resulting intrusion map for each settlement was then summed to account for typical overlaps of intrusion from nearby settlements. We assumed that there is a limit at very high population densities, and so we capped the maximum value of intrusion, X, at 1,000,000 then max-normalized using a square-root transform:

$$F_i = X^{0.5} * 0.001 \quad , \tag{23}$$

$$H_i = F_i * p(C_i) * I_i \quad . \tag{24}$$

Note that accessibility was calculated using estimates of travel time along roads and rails, as well as off-road through different features of the landscape, using established travel time factors (Tobler 1991) and presuming walking off-trail or via boats on freshwater or along ocean shoreline (Nelson 2008; Theobald et al. 2010; Weiss et al. 2018; Nelson et al. 2019). This included effects of international borders following Weiss et al. (2018), and accessibility to lands was calculated across oceans.

2.2.10 Natural systems modification

Dams and their associated reservoirs flood natural habitat and strongly impact the natural flow regimes of the adjacent rivers (Grill et al. 2019). We mapped the footprint of reservoirs F_r created from 6,849 dams from the Global Reservoirs and Dams database (GRanD v1.3; Lehner et al. 2011; http://globaldamwatch.org/grand/).

$$H_r = F_r * p(C_r) * I_r \quad . \tag{25}$$

Because there are some potential analyses that would benefit from treating all water bodies consistently, we provided an additional version with all water bodies masked out in the dataset.

2.2.11 Pollution

We estimated the stress of air pollution by using data on nitrogen oxides (NO_x) through time from the Emissions Database for Global Atmospheric Research (EDGAR v4.3.2; Crippa et al. 2018). We selected NO_x because it is a strong contributor to acid rain/fog and tropospheric ozone and because atmospheric levels are predominantly from human-sources (Delmas et al. 1997). We used the 99th percentile (46,750 M tonnes) as the maximum value and then max-normalized (F_{nox}) and adjusted using the intensity value I_{nox} :

$$H_{nox} = F_{nox} * p(C_{nox}) * I_{nox} \quad . \qquad (26)$$

2.3 Uncertainty and validation analyses

To understand the uncertainty of our results associated with our estimated intensity values (Table 2), following Kennedy et al. (2019b), we re-calculated *H* where I_s was randomized (n=50) between the minimum and maximum intensity values ~~(at 1 km² resolution for computational efficiency). We quantified the mean and standard deviation of the resulting global *H* values for n=50 randomizations.~~for each stressor. We then calculated the per-pixel mean and standard deviation for the 50 randomizations at 1 km² resolution for computational efficiency and provide corresponding maps.

We also assessed the accuracy of our maps following validation procedures described in Kennedy et al. (2019a, 2019b, 2019c). Because historical "ground truth" human modification data in comparable form are not widely available, we restricted our analysis to test the contemporary ~~(~2017) conditions map of human modification~~conditions of human modification (~2017 map) that included all stressor layers. We used ~~the validation data~~an independent validation dataset from Kennedy et al. (2019a)~~, which is an independent validation dataset~~ that quantified the degree of human modification from visual interpretation of high resolution aerial or satellite imagery across the world. We selected plots using the Global Grid sampling design (Theobald 2016), a spatially-balanced and probability-based random sampling that was stratified on a five-class rural to urban gradient using "stable nighttime-lights" 2013 imagery (Elvidge *et al.*, 2001). Within each of 1,000 ~1 km² plots, we selected 10 simple-random locations to capture rare features and heterogeneity in land use and land cover (for a total of 10,000 sub-plots), which were separated by a minimum distance of 100 m. The spatial-balanced nature of the design maximizes statistical information extracted from each plot, because it increases the number of samples in relatively rare areas that are likely of interest (in contrast to simple random sampling) -- especially for urbanized and growing cities (Theobald, 2016).

2.4 Processing platform

We processed, modeled, and analyzed the spatial data using the Google Earth Engine platform (Gorelick et al. 2017). We calculated all distances and areas using geodesic algorithms in decimal degrees (EPSG: 4326). We summarized areas and percentages after projecting the data to Mollweide equal-area (WGS84) to simplify calculations. All datasets and maps conform to the Google Earth Engine terms of service. We used program R 3.6.1 (R Core Team 2019) to generate Fig. 2.

3 Results

Below we describe the temporal and spatial trends of human modification by continents (Table 4), biomes (Table 5), and ecoregions (Fig. 2).

3.1 Changes from 1990-2015

The mean value of *H* for global terrestrial lands increased from ~~0.08221~~0.0822 in 1990 to ~~0.09458~~0.0946 in 2015, a percentage change of 15.04% ~~(~~overall and 0.60% annually~~;~~ (Table 4). This equates to 1.6 M km^2 of natural lands lost -- ~~roughly 177~~178 km^2 daily ~~or 17 football pitches per minute (i.e. an international football field)~~. Increases in human modification occurred ~~across the globe and across~~globally and in both urban and rural locations. We found that the largest increases in H_{mad} occurred in Oceania, followed by Asia and Europe. Australia had the lowest increase followed by North and South America (Table 4). The biomes that exhibited the greatest increases in modification were mangroves; tropical & subtropical moist broadleaf forests; and tropical & subtropical dry broadleaf forests; while the biomes with the smallest increases were tundra; boreal forests/taiga; and deserts and xeric shrublands. Maps of changes in H_{mad} between 2015 and 1990 for each ecoregion are shown in Fig. 1a, relative to HF (Fig. 1b) and THPI (Fig. 1c). Figure 2 shows the ratio of natural land loss between 1990 and 2015, for each ecoregion and grouped by biome, in the context of the contemporary extent of human modification. We found most ecoregions (*n*=814) had increased in human modification, while the few (*n*=32) that had decreased were concentrated in higher latitudes and in more remote areas. We also found that changes in H_{mad} have increased over time, from ~~0.00042 to 0.00051 to 0.00062~~0.0004 to 0.0005 to 0.0006, during 1990-2000 to 2000-2010 to 2010-2015. The percent change has also increased over time from 0.51% to 0.59% to 0.68%.

3.2 Contemporary extent

We found that about 19.1 M km^2 (±0.0013) of natural lands were lost by ~2017 -- about 14.6% of land globally (Table 4). South America was the most transformed (28.7%), followed by North America (16.8%), while Australia (5.0%) and Africa (10.7%) were the least transformed. Broad-scale patterns of the extent of human modification in ~2017 are shown in Fig. 3. Note that "natural lands lost" was calculated using the continuous value of *H*, rather than approximations based on classifying the distribution.

Terrestrial lands with very low levels of human modification (*H*<0.01; Kennedy 2009c, Riggio et al. 2020) are concentrated in less productive and more remote areas in high latitudes and dominated by inaccessible permanent rock and ice or within tundra, boreal forests, desert regions, and to a lesser extent montane grasslands. Table 5 shows that the biomes with the highest levels of *H* in ~2017 were temperate broadleaf and mixed forests (*H*=~~0.37435~~0.3744); tropical & subtropical dry broadleaf forests (*H*=~~0.33170~~0.3317); and Mediterranean forests, woodlands & scrub (*H*=~~0.29027~~0.2903). The five least modified biomes were tundra (mean *H*=~~0.00230~~0.0023); boreal forests/taiga

(H=~~0.02129~~0.0213); deserts and xeric shrublands (H=~~0.05706~~0.0572); and montane grasslands and shrublands (H=~~0.08943~~0.0894).

~~We~~Following thresholds from Kennedy et al. (2019a), we found that in ~2017, 51.0% of global lands had ~~very low human modification (mean $H \leq 0.01$; 66.8 M km^2~~a mean value $H \leq 0.01$ (i.e. very low human modification,), 13.3% had ~~low human modification (~~a mean of $0.01 < H \leq 0.1$~~; 17.4 M km^2), 21.0% had moderate human modification (~~ (low) , 21.0% had a mean of $0.1 < H \leq 0.4$~~; 27.6 M km^2~~ (i.e. moderate), 12.3% had ~~high human modification (~~a mean value of $0.4 < H \leq 0.7$~~; 16.1 M km^2~~ (high), and 2.4% ~~had very high human modification ($0.7 < H \leq 1.0$; 3.2 M km^2) (following the thresholds from Kennedy et al. 2019a). We found that ~4.2% of lands have no evidence of human modification ($H <$ 0.00001; 5.5 M km^2), based on our estimate of the level of precision (~0.00001) given the data inputs.~~ (3.2 M km^2, ±0.0003) had a mean of $0.7 < H \leq 1.0$ (very high). By area, these results by class amount to: very low=66.8 M km^2 (±0.0067), low=17.4 M km^2 (±0.0017), moderate= 27.6 M km^2 (±0.0028), high=16.1 M km^2 (±0.0016), and very high=3.18 M km^2, ±0.0003). Also, we found that 17.6% had a mean value of $H < 0.0001$ (23.0 M km^2, ±0.0023), and 4.2% had $H < 0.00001$ (5.5 M km^2, ±0.0006).

3.3 Comparisons

We compared our work to earlier efforts (summarized in Table 6) to determine if overall trends and extents were generally consistent and ~~resulting~~with similar priorities of biomes and ecoregions ~~were similar~~. Globally, H_{mad} from 1990-2015 (t=1990, u=2015) was ~~0.00049~~0.0005, while for HF and THPI it was higher (HF_{mad}=~~0.00056~~0.0006, $THPI_{mad}$=~~0.00081~~0.0008). Perhaps more important is that the variability of the mean annualized difference values in the HF and THPI was 2.3 and 3.2 times that of ~~HM~~*H*. By continent, we found that H_{mad} increased the most in Oceania, followed by Asia, Europe, Africa, South America, North America, and Australia. Continental ranks by THPI followed ~~HM~~H roughly, though HF differed more substantially (Table 5). H_{mad} increased for all continents, but HF_{mad} showed *declines* in modification for Europe and South America, while $THPI_{mad}$ showed a decline for North America.

We also found the ranking of biomes by mean annualized difference for HF and THPI were fairly different from ~~HM ranks~~ranks developed from H values (Table ~~6~~7). Of the three biomes with the largest increase for H_{mad}, two ~~of them~~ were also identified by HF (tropical & subtropical dry broadleaf forests and tropical & subtropical moist broadleaf forests) and none ~~of them by~~ THPI. Of the five biomes with the largest increase for H_{mad}, three ~~of them~~ were also identified by HF and THPI. The biomes that had the greatest disagreement amongst the ranking of ~~HM~~H, HF, and THPI were mangroves; tropical & subtropical coniferous forests; and tropical & subtropical dry broadleaf forests. ~~The results for ecoregions shown in Fig. 1 are even more striking, as the mean annualized difference values for HF and THPI were inconsistent with HM results. Of the 814 ecoregions that had increases in H_{mad}, a decrease in modification was found for 201 ecoregions in HF_{mad} and 202 for $THPI_{mad}$; and for the 32 ecoregions that were found to have decreases in H_{mad}, an increase in modification was found for 20 in HF and 22 in THPI. (Note that data layers can be viewed here).~~

~~In terms of the overall amount of recent (~2017) human modification globally, we found that 14.5% of terrestrial lands globally have been modified -- which is roughly similar to HF (12.3% for ~2009; Venter et al. 2016) and the degree of human modification at 1-km resolution (HM1k; 19% for ~2016; Kennedy et al. 2019a)~~

The biggest differences in rankings between the H and the HF were for temperate and broadleaf mixed forests (and see comparisons of H1k and HF in Kennedy et al. 2019a, 2019b, Riggio et al. 2020). HF was estimated to result in 12.3% modification for an earlier date (~2009; Venter et al. 2016) and is lower likely because fewer stressors were included, its additive combination method, and its strongly right-skewed distribution caused by max-value normalization. The ranks of the extent of modification by biomes, however, were very similar between ~~HM, HM1k~~H, H1k, and HF. In general, ~~the HM~~H had intermediate modification levels compared to ~~HM1k~~H1k and HF: with ~~HM1k~~H1k levels being slightly higher (difference between 0.00 min to 0.09 and average difference of 0.05 by biome) and HF being slightly lower (difference between 0.00 min to 0.13 max and average difference of 0.04 by biome~~) (Table 6). The~~; Table 7). Results for ecoregions shown in Fig. 1 are even more striking, as the mean annualized difference values for HF and THPI were inconsistent with our results. Of the 814 ecoregions that had increases in H_{mad}, a decrease in modification was found for 201 ecoregions in HF_{mad} and 202 for $THPI_{mad}$; and for the 32 ecoregions that were found to have decreases in H_{mad}, an increase in modification was found for 20 in HF and 22 in THPI.

Finally, the global estimate for ~~HM1k~~H1k was likely higher than ~~HM because HM1k~~H because H1k did not limit the livestock stressor at LU km^{-2} <1.0, used a slightly higher value for the low-threshold on the electrical infrastructure and energy use stressor (i.e. "nightlights"), and reported results that incorporate uncertainty in estimates of intensity. ~~The biggest differences in rankings between the HM and the HF were for temperate and broadleaf mixed forests (and see comparisons of HM1k and HF in Kennedy et al. 2019a, 2019b~~Furthermore, global modification from farming was estimated at 37% for 2000 (Ramankutty et al. 2008) compared to 14.6% with H. The difference with our results is largely due to their mapping of the area land cover types but not differentiating the intensity of the impact of those cover types (crop and pasture).

3.4 Uncertainty and validation analyses

~~To examine the uncertainty associated with our intensity estimates, we calculated across all terrestrial lands the mean *H* value on datasets generated with intensity values drawn from a uniform random distribution between the minimum and maximum estimates. We generated 50 randomized datasets and found the mean of the randomized maps was 0.14306 and the standard deviation was ±0.00106 (compared to~~We addressed uncertainty in our results by incorporating the parameter $p(C_s)$ for every sector *s* to best quantify uncertainty in its spatial location and classification as detailed in section 2.2.; for example, we adjusted $p(C_{cp})$ by directly incorporating measured confusion among land cover types using the results from the accuracy assessment of the land cover dataset (from Eq. 4). Additionally, we incorporated uncertainty by calculating the global mean for each of the 50 randomizations, which across the 50 iterations was 0.1434 (SD= ±0.0076) and ranged from 0.1243 to 0.1612. Thus, the global mean of 0.1461 obtained using our "best-estimate~~ of 0.14605). The lowest~~

~~possible mean *H* value calculated with the minimum estimate for all stressors was 0.10686 and the highest possible value using the maximum estimate was 0.18493.~~" intensity values was in line with our uncertainty results. We also mapped the per-pixel variance (standard deviation) to examine the spatial pattern of uncertainty (Figure 4). The locations of the highest levels of uncertainty tend to be in more highly developed landscapes.

We found strong agreement between ~~our ~2017 HM dataset~~*H* for ~2017 and our validation data (r=0.783), with an average root-mean-square-error of 0.22 and a mean-absolute-error of 0.04, for the 926 ~1 km^2 plots (9,260 sub-plots). There were 726 plots within ±20% agreement, while for 161 plots *H* was estimated higher than our visual estimate from the validation data (and 39 plots lower). Estimates of *H* were biased high, likely because the stressors for the "human intrusion" and electrical infrastructure (based on nighttime lights) are not readily observable from the aerial imagery used to generate the validation data.¶
Our results here are consistent with our earlier findings (Kennedy et al. 2019a, 2019b, 2019c).

4 Discussion

4.1 Summary

We found rapid and increasing human modification of terrestrial systems, resulting in the loss of natural lands globally. Our findings foreshadow trends and patterns of increased human modification, assuming future trends in the next 25-30 years continue as they have recently. Thus, our study reinforces calls for stronger commitments to help reduce habitat loss and fragmentation (Kennedy et al. 2019a, Jacobson et al. 2019) -- which should be considered in conjunction with current commitments ~~(e.g.,~~ to reduce CO_2 emissions through the Paris climate accord~~;~~ (Baruch-Mordo et al. 2019; Kiesecker et al. 2019). We believe that the comparisons of ecoregions and biomes ~~shown in Fig. 2~~ offer valuable contextual information that provides initial guidance on conservation strategies that may be most appropriate (Kennedy et al. 2019a). Also, it is important to consider the ~~relative importance of each ecoregion towards meeting representation goals by ecoregion~~feasibility of achieving ecoregional (Dinerstein et al. 2017) or ecosystem (Jantke et al. 2019) representation goals, as well as ~~considering~~ additional stresses caused by climate change (Costanza and Terando 2019). We emphasize that although global, continental, biome, and ecoregional summaries provide a general ~~idea~~understanding of trends and patterns, ~~our work here supports robust estimates at country and within ecoregional patterns of the gradient of human modification~~the high resolution of *H* and its gradient nature supports robust estimates of change in human modification within a country and within an ecoregion, which are essential for tracking progress toward international and national conservation commitments (Mace et al. 2018), especially when placed within a broader structured decision~~-~~-making framework (Tullock et al. 2015)

Our datasets of human modification provide the most granular, contemporary, comprehensive, high-quality, and robust data currently available to assess temporal and spatial trends of global human ~~modification~~impacts on landscapes. Our work is grounded in a structured classification of stressors, uses an internally-consistent model, evaluates uncertainty, and incorporates refinements to minimize the effects of scaling and classification errors. Our validation approach uses an independent and spatially-balanced random sample design to provide strong support for the quality of our findings (Kennedy et al. 2019c).

Our overarching goal in producing and publishing these datasets is to support detailed quantification of the rates and trends, as well as the current extent and pattern, and to understand the ~~gradient of the~~ degree of human modification across the continuum from low (e.g., wilderness) to high (e.g., intense urban). Beyond the basic findings presented here, we believe there are many potential applications of these datasets, including: examining temporal rates and trends of land modification in and around protected areas (e.g., Geldmann et al. 2019a); estimating fragmentation for ~~all~~ ecoregions and biomes (Kennedy et al. 2019a, Jacobson et al. 2019); and evaluating conservation opportunities and risks (e.g., the conservation risk index; Hoekstra et al. 2005). We also note that the human modification approach allows, in a straightforward and logically consistent way, inclusion of additional stressors and higher resolution datasets that may become available over time or may be available for specific, local areas.

4.2 Caveats

As with any model, we recognize there are limitations of our work. We did not include data for all human stressors, ~~typically~~largely because of incomplete global coverage or ~~too~~ coarse mapping units (Klein Goldewijk et al. 2007; Geldmann *et al.*, 2014), an inability to discern human-induced versus natural disturbances ~~(e.g., wildfires)~~, or uncertainty in the location and directionality of its impact (e.g.; climate change on terrestrial systems; Geldmann *et al.*, 2014). ~~Although our datasets described here have order-of-magnitude higher resolution than previous temporal maps, estimates of *H* generated for areas less than roughly 100 km² should be used with caution.~~ In particular and discussed in Kennedy et al. (2019a, 2019b), changes to land cover due to ecological disturbance events, such as wildfires or flooding, are not included in our analysis because of the difficulty in separating natural from human-caused disturbances -- yet, we recognize that the broad extent of wildfire in particular, could have strong implications. We did not include climate data as a stressor in this product to keep our analysis manageable and tractable. For more integrated analyses, our data product should be used in combination with datasets of impacts due to climate change (e.g., Parks et al. 2020).

Stressors that are particularly important to improve include effects of grazing (currently coarse data and very broad expanse), pasture land, invasive species, and climate change (especially wildfire and effects of sea-level rise), and we encourage future work to focus on developing appropriate datasets and approaches to include or better capture these stressors. Key datasets we believe should be improved include transportation networks, including logging roads (e.g., Van Etten 2019) that are comparable through time; livestock grazing, rangelands, croplands, timber plantations, and pasturelands and their intensity of use; resource extraction (especially mining footprints); and temporal trends in gas flares, utility-scale solar ~~plants, electrical substations, etc.~~

4.3 Data availability

The datasets generated from this work are available here (Figshare DOI pending). All other datasets used in our work are open-source data and are listed below.

Center for International Earth Science Information Network: Global Rural-Urban Mapping Project, Version 1 (GRUMPv1): Settlement Points, Revision 01. Palisades, NY: NASA Socioeconomic Data and Applications Center (SEDAC). https://doi.org/10.7927/H4BC3WG1, 2017, Accessed 1 January 2019.

Center for International Earth Science Information Network: Gridded Population of the World, Version 4 (GPWv4): Administrative Unit Center Points with Population Estimates, Revision 11. Palisades, NY: NASA Socioeconomic Data and Applications Center (SEDAC). https://doi.org/10.7927/H4BC3WMT, 2018, Accessed 1 January 2019.

Corbane, C., Florczyk, A., Pesaresi, M., Politis, P., Syrris, V.: GHS built-up grid, derived from Landsat, multitemporal (1975-1990-2000-2014), R2018A. European Commission, Joint Research Centre (JRC) doi: 10.2905/jrc-ghsl-10007 PID: http://data.europa.eu/89h/jrc-ghsl-10007, 2018

Crippa, M., Guizzardi, D., Muntean, M., Schaaf, E., Dentener, F., van Aardenne, J. A., Janssens-Maenhout, G.: Gridded emissions of air pollutants for the period 1970–2012 within EDGAR v4. 3.2. Earth System Science Data, 10(4), 1987-2013, https://data.jrc.ec.europa.eu/collection/EDGAR, 2018.

Curtis, P.G., Slay, C.M., Harris, N.L., Tyukavina, A., Hansen, M.C.: Classifying drivers of global forest loss. Science, 361(6407), pp.1108-1111, https://science.sciencemag.org/content/sci/suppl/2018/09/12/361.6407.1108.DC1, 2018.

Elvidge, C., Ziskin, D., Baugh, K., Tuttle, B., Ghosh, T., Pack, D., Erwin, E., Zhizhin, M.: A Fifteen Year Record of Global Natural Gas Flaring Derived from Satellite Data. Energies 2 (3): 595, doi:10.3390/en20300595. https://payneinstitute.mines.edu/eog/dmsp/, 2009.

Geldmann, Jonas; Joppa, Lucas; Burgess, Neil D.: Temporal Human Pressure Index, v2, Dryad, Dataset, https://doi.org/10.5061/dryad.p8cz8w9kf, 2019b.

Gilbert, M., Nicolas, G., Cinardi, G., Van Boeckel, T. P., Vanwambeke, S. O., Wint, G. W., Robinson, T. P. Global distribution data for cattle, buffaloes, horses, sheep, goats, pigs, chickens and ducks in 2010. Scientific Data, 5, 180227, https://doi.org/10.7910/DVN/BLWPZN, https://doi.org/10.7910/DVN/33N0JG, https://doi.org/10.7910/DVN/7Q52MV, https://doi.org/10.7910/DVN/OCPH42, https://doi.org/10.7910/DVN/ICHCBH, https://doi.org/10.7910/DVN/GIVQ75, https://doi.org/10.7910/DVN/SUFASB, https://doi:10.7910/DVN/5U8MWI, 2018.

Hansen, M. C., Potapov, P. V., Moore, R., Hancher, M., Turubanova, S. A. A., Tyukavina, A., Kommareddy, A.: High-resolution global maps of 21st-century forest cover change. Science, 342(6160), 850-853, http://earthenginepartners.appspot.com/science-2013-global-forest., 2013.

Kehoe, L., Romero-Muñoz, A., Polaina, E., Estes, L., Kreft, H., Kuemmerle, T.: Biodiversity at risk under future cropland expansion and intensification. Nature Ecology & Evolution, 1(8), 1129, doi:10.1038/s41559-017-0234-3, 2017.

~~Kennedy, C.M., Oakleaf, J., Theobald, D.M., Baruch-Mordo, S., Kiesecker, J.: Global Human Modification. figshare. Dataset. https://doi.org/10.6084/m9.figshare.7283087.v1, 2018.¶~~

~~Li, W., MacBean, N., Ciais, P., Defourny, P., Lamarche, C., Bontemps, S., Houghton, R. A., and Peng, S.: Gross and net land cover changes in the main plant functional types derived from the annual ESA CCI land cover maps (1992–2015), Earth Syst. Sci. Data, 10, 219-234, https://doi.org/10.5194/essd-10-219-2018, 2018.¶~~

~~OpenStreetMap contributors: Planet dump [Data file from April 27, 2019]. Retrieved from https://planet.openstreetmap.org, 2019.¶~~

~~UNEP-WCMC and IUCN: Protected Planet: The World Database on Protected Areas (WDPA). www.protectedplanet.net, July 2019, Cambridge, UK, 2019.¶~~

~~Venter, O., Sanderson, E.W., Magrach, A., Allan, J.R., Beher, J., Jones, K.R., Possingham, H.P., Laurance, W.F., Wood, P., Fekete, B.M., Levy, M.A., Watson, J.E.M.: Global terrestrial Human Footprint maps for 1993 and 2009. Sci. Data 3:160067. DOI: 10.1038/sdata.2016.67, 2016.¶~~

~~Waldner, F., Fritz, S., Di Gregorio, A., Plotnikov, D., Bartalev, S., Kussul, N., Löw, F.: A unified cropland layer at 250 m for global agriculture monitoring. https://dx.doi.org/10.6084/m9.figshare.20166752, 2016.¶~~

~~WRI. Global Energy Observatory, Google, KTH Royal Institute of Technology in Stockholm, Enipedia, World Resources Institute. 2019. Global Power Plant Database. http://resourcewatch.org. Accessed 14 April 2019.¶~~

and wind installations (Dunnett et al. 2020), and electrical substations.

4.3 Data availability

The datasets generated from this work are available at https://doi.org/10.5061/dryad.n5tb2rbs1 (Theobald et al. 2020), which includes the land/water mask used to support subsequent analyses. Extracts of specific geographic areas can be obtained by contacting the authors. All other datasets used in our work are open-source data cited within.

Author contributions

DT, CK, BC, JO, SBM, JK conceived the paper; DT, CK, JO, BC prepared data; DT implemented the model; DT, CK, BC, SBM conducted summary analyses; DT, CK, BC, JO, SBM, JK developed recommendations; all contributed to writing the manuscript.

Competing interests~~.~~: The authors declare that they have no conflict of interest.

Acknowledgments

We thank OpenStreetMap contributors (copyright OpenStreetMap and data are available from https://www.openstreetmap.org), and E. Lebre for assistance with the global mining data.

References

Allred, B. W., Smith, W. K., Tidwell, D., Haggerty, J.H., Running, S. W., Naugle, D.E., Fuhlendorf, S.D.: Ecosystem services lost to oil and gas in North America. Science, 348(6233):401-402, 2015.

Alonso, W.: A theory of the urban land market. Papers in Regional Science, 6(1), 149-157, 1960.

van Asselen, S., Verburg, P. H.: A Land System representation for global assessments and land-use modeling. Global Change Biology, 18(10), 3125-3148, 2012.

Baruch-Mordo, S., Kiesecker, J., Kennedy, C.M., Oakleaf, J.R. and Opperman, J.J.: From Paris to practice: sustainable implementation of renewable energy goals. Environmental Research Letters. https://iopscience.iop.org/article/10.1088/1748-9326/aaf6e0, 2019.

Bonham-Carter, G.F.: Geographic information systems for geoscientists: modelling with GIS (Vol. 13), Elsevier, 2014.

Brown, M. T., Vivas, M. B.: Landscape development intensity index. Environmental Monitoring and Assessment, 101(1-3), 289-309, 2005.

Center for International Earth Science Information Network - CIESIN - Columbia University, CUNY Institute for Demographic Research - CIDR, International Food Policy Research Institute - IFPRI, The World Bank, and Centro Internacional de Agricultura Tropical - CIAT.: Global Rural-Urban Mapping Project, Version 1 (GRUMPv1): Settlement Points, Revision 01. Palisades, NY: NASA Socioeconomic Data and Applications Center (SEDAC). https://doi.org/10.7927/H4BC3WG1, 2017, Accessed 1 January 2019.

Center for International Earth Science Information Network - CIESIN - Columbia University. Gridded Population of the World, Version 4 (GPWv4): Administrative Unit Center Points with Population Estimates, Revision 11. Palisades, NY: NASA Socioeconomic Data and Applications Center (SEDAC). https://doi.org/10.7927/H4BC3WMT, 2018, Accessed 1 January 2019.

Chaudhary, A. Brooks, T.M.: Land use intensity-specific global characterization factors to assess product biodiversity footprints. Environmental Science & Technology, 52(9), 5094-5104, 2018.

Corbane, C., Florczyk, A., Pesaresi, M., Politis, P., Syrris, V.: GHS built-up grid, derived from Landsat, multitemporal (1975-1990-2000-2014), R2018A. European Commission, Joint Research Centre (JRC) doi: 10.2905/jrc-ghsl-10007 PID: http://data.europa.eu/89h/jrc-ghsl-10007, 2018

Costanza, J.K., Terando, A.J.: Landscape Connectivity Planning for Adaptation to Future Climate and Land-Use Change. *Current Landscape Ecology Reports*, *4*(1), pp.1-13, 2019.

Crippa, M., Guizzardi, D., Muntean, M., Schaaf, E., Dentener, F., van Aardenne, J. A., Janssens-Maenhout, G.: Gridded emissions of air pollutants for the period 1970–2012 within EDGAR v4. 3.2. Earth System Science Data, 10(4), 1987-2013, 2018.

Curtis, P.G., Slay, C.M., Harris, N.L., Tyukavina, A., Hansen, M.C.: Classifying drivers of global forest loss. Science, 361(6407), pp.1108-1111, https://science.sciencemag.org/content/sci/suppl/2018/09/12/361.6407.1108.DC1, 2018.

Delmas, R., Serca, D., Jambert, C.: Global inventory of NOx sources. Nutrient cycling in Agroecosystems, 48(1-2), 51-60, 1997.

Demographia. Demographia World Urban Areas 12th Annual Edition. pp 110, http://www.demographia.com/db-worldua.pdf, 2016.

Dinerstein, E., Olson, D., Joshi, A., Vynne, C., Burgess, N.D., Wikramanayake, E., Hahn, N., Palminteri, S., Hedao, P., Noss, R., Hansen, M.: An ecoregion-based approach to protecting half the terrestrial realm. BioScience, 67(6), 534-545, 2017.

Dinerstein, E., Vynne, C., Sala, E., Joshi, A. R., Fernando, S., Lovejoy, T. E., Burgess, N. D.: A Global Deal For Nature: Guiding principles, milestones, and targets. Science Advances, 5(4), eaaw2869, 2019.

Ellis, E. C., Ramankutty, N.: Putting people in the map: anthropogenic biomes of the world. Frontiers in Ecology and the Environment, 6,8: 439-447, 2008.

Ellis, E.: *Anthropocene: A very short introduction*. Oxford University Press. Oxford, UK. 2018.

Elvidge, C.D., Imhoff, M.L., Baugh, K.E.: Night-time lights of the world: 1994–1995. ISPRS Journal of Photogrammetry and Remote Sensing, 56, 81-99, 2001.

Elvidge, C., Ziskin, D., Baugh, K., Tuttle, B., Ghosh, T., Pack, D., Erwin, E., Zhizhin, M.: A Fifteen Year Record of Global Natural Gas Flaring Derived from Satellite Data. Energies 2 (3): 595, doi:10.3390/en20300595, 2009.

Elvidge, C. D., Baugh, K. E., Zhizhin, M., Hsu, F. C.: Why VIIRS data are superior to DMSP for mapping nighttime lights. Proceedings of the Asia-Pacific Advanced Network, 35(0), 62, 2013.

Elvidge, C., Zhizhin, M., Baugh, K., Hsu, F. C., & Ghosh, T.: Methods for global survey of natural gas flaring from visible infrared imaging radiometer suite data. Energies, 9(1), 14, 2016.

ESA CCI. Land Cover CCI Product User Guide v2 (CCI-LC-PUGv2). Table 3-6, 2017.

Esteves, C.F., de Barros Ferraz, S.F., de Barros, K.M., Ferraz, M.G., Theobald, D.M.: Human accessibility modelling applied to protected areas management. Natureza & Conservacao, 9(2):232-9, 2011.

van Etten, A.: City-scale road extraction from satellite imagery. arXiv:1904.09901v2 [cs.CV] 22 Jul 2019.

Fritz, S., See, L., Perger, C., McCallum, I., Schill, C., Schepaschenko, D., Lesiv, M.: A global dataset of crowdsourced land cover and land use reference data. Scientific Data, 4, 170075, 2017.

Gardner, R. H., Urban, D. L.: Neutral models for testing landscape hypotheses. Landscape Ecology, 22(1), 15-29, 2007.

Geldmann, J., Joppa, L. N., Burgess, N.D.: Mapping change in human pressure globally on land and within protected areas. Conservation Biology, 28(6), 1604-1616, 2014.

Geldmann, J., Manica, A., Burgess, N.D., Coad, L., Balmford, A.: A global-level assessment of the effectiveness of protected areas at resisting anthropogenic pressures. Proceedings of the National Academy of Sciences, 116(46), 23209-23215, 2019a.

Geldmann, J., Joppa, L., Burgess, N.D.: Temporal Human Pressure Index, v2, Dryad, Dataset, https://doi.org/10.5061/dryad.p8cz8w9kf, 2019b.

Gerber, P., Mooney, H.A., Dijkman, J., Tarawal, S., De Haan, C.: Livestock in a Changing Landscape, Volume 2: Experiences and Regional Perspectives, Washington, D.C., Island Press, 2010.

Gilbert, M., Nicolas, G., Cinardi, G., Van Boeckel, T. P., Vanwambeke, S. O., Wint, G. W., Robinson, T. P.: Global distribution data for cattle, buffaloes, horses, sheep, goats, pigs, chickens and ducks in 2010. Scientific Data, 5, 180227, ~~2018~~2018a.

Gilbert, M., Nicolas, G., Cinardi, G., Van Boeckel, T. P., Vanwambeke, S. O., Wint, G. W., Robinson, T. P. Global distribution data for cattle, buffaloes, horses, sheep, goats, pigs, chickens and ducks in 2010. Scientific Data, 5, 180227, https://doi.org/10.7910/DVN/BLWPZN, https://doi.org/10.7910/DVN/33N0JG, https://doi.org/10.7910/DVN/7Q52MV, https://doi.org/10.7910/DVN/OCPH42, https://doi.org/10.7910/DVN/ICHCBH, https://doi.org/10.7910/DVN/GIVQ75, https://doi.org/10.7910/DVN/SUFASB, https://doi:10.7910/DVN/5U8MWI, 2018b.

González-Abraham, C., Ezcurra, E., Garcillán, P. P., Ortega-Rubio, A., Kolb, M., Creel, J. E. B.: The human footprint in Mexico: physical geography and historical legacies. PloS ONE, 10(3), e0121203, 2015.

Gorelick, N., Hancher, M., Dixon, M., Ilyushchenko, S., Thau, D., Moore, R. Google Earth Engine: Planetary-scale geospatial analysis for everyone. *Remote Sensing of Environment*, *202*, pp. 18-27, 2017.

Grill, G., Lehner, B., Thieme, M., Geenen, B., Tickner, D., Antonelli, F., Macedo, H. E.: Mapping the world's free-flowing rivers. Nature, 569(7755), 215, 2019.

Haddad, N. M., Brudvig, L. A., Clobert, J., Davies, K. F., Gonzalez, A., Holt, R. D., Cook, W. M.: Habitat fragmentation and its lasting impact on Earth's ecosystems. Science Advances, 1(2), e1500052, 2015.

Hajkowicz, S., Collins, K.: A review of multiple criteria analysis for water resource planning and management. Water Resources Management, *21*(9), pp.1553-1566, 2007.

Halpern, B.S., Mcleod, K.L, Rosenberg, A.A., Crowder, L.B.: Managing for cumulative impacts in ecosystem-based management through ocean zoning. Ocean & Coastal Management 51, 203-211, 2008.

Halpern, B.S., Fujita, R.: Assumptions, challenges, and future directions in cumulative impact analysis. Ecosphere, 4, 1-11, 2013.

Hansen, M. C., Potapov, P. V., Moore, R., Hancher, M., Turubanova, S. A. A., Tyukavina, A., Kommareddy, A.: High-resolution global maps of 21st-century forest cover change. Science, 342(6160), 850-853, 2013.

Hoekstra, J.M., Boucher, T.M., Ricketts, T.H.,Roberts, C.: Confronting a biome crisis: global disparities of habitat loss and protection. Ecology Letters, 8(1), pp.23-29, 2005.

Hurtt, G. C., Frolking, S., Fearon, M. G., Moore, B., Shevliakova, E., Malyshev, S., . . . Houghton, R. A.: The underpinnings of land-use history: three centuries of global gridded land-use transitions, wood-harvest activity, and resulting secondary lands. Global Change Biology, 12(7), 1208–1229. https://doi.org/10.1111/j.1365- 2486.2006.01150.x, 2006.

IPBES. Summary for policymakers of the global assessment report on biodiversity and ecosystem services of the Intergovernmental Science-Policy Platform on Biodiversity and Ecosystem Services. S. Díaz, J. Settele, E. S. Brondizio E.S., H. T. Ngo, M. Guèze, J. Agard, A. Arneth, P. Balvanera, K. A. Brauman, S. H. M. Butchart, K. M. A. Chan, L. A. Garibaldi, K. Ichii, J. Liu, S. M. Subramanian, G. F. Midgley, P. Miloslavich, Z. Molnár, D. Obura, A. Pfaff, S. Polasky, A. Purvis, J. Razzaque, B. Reyers, R. Roy Chowdhury, Y. J. Shin, I. J. Visseren-Hamakers, K. J. Willis, and C. N. Zayas (eds.). IPBES secretariat, Bonn, Germany, 2019.

IPCC: Climate change and land: summary for policymakers. URL: https://www.ipcc.ch/report/srccl/, 2019. Accessed November 21, 2019.

Jacobson, A.P., Riggio, J., Tait, A., Baillie, J.: Global areas of low human impact ('Low Impact Areas') and fragmentation of the natural world. *Scientific Reports*, 2019.

Jantke, K., Kuempel, C.D., McGowan, J., Chauvenet, A.L., Possingham, H.P.: Metrics for evaluating representation target achievement in protected area networks. *Diversity and Distributions*, 25(2), pp.170-175, 2019.

Jordan, M., Meyer, W. B., Kates, R. W., Clark, W. C., Richards, J. F., Turner, B. L., Mathews, J. T.: *The earth as transformed by human action: global and regional changes in the biosphere over the past 300 years*. CUP Archive, 1990.

Kehoe, L., Romero-Muñoz, A., Polaina, E., Estes, L., Kreft, H., Kuemmerle, T.: Biodiversity at risk under future cropland expansion and intensification. Nature Ecology & Evolution, 1(8), 1129, doi:10.1038/s41559-017-0234-3, 2017.

Kiesecker, J., Baruch-Mordo, S., Kennedy, C.M., Oakleaf, J.R., Baccini, A. and Griscom, B.W.: Hitting the Target but Missing the Mark: Unintended Environmental Consequences of the Paris Climate Agreement. *Frontiers in Environmental Science*, https://doi.org/10.3389/fenvs.2019.00151, 2019.

Kennedy, C.M., Oakleaf, J.R., Theobald, D.M., Baruch-Mordo, S., Kiesecker, J.: Managing the middle: A shift in conservation priorities based on the global human modification gradient. Global Change Biology, 25(3), 811-826, 2019a.

Kennedy, C.M., Oakleaf, J.R., Theobald, D.M., Baruch-Mordo, S., Kiesecker, J.: Supplementary information for: Managing the middle: A shift in conservation priorities based on the global human modification gradient. Global Change Biology, 25(3), 811-826, 2019b.

Kennedy, C.M., Oakleaf, J.R., Baruch-Mordo, S., Theobald, D.M. & Kiesecker, J.: Finding middle ground: Extending conservation beyond wilderness areas. Global Change Biology doi:10.1111/gcb.14900, 2019c.

Kennedy, C.M., Oakleaf, J., Theobald, D.M., Baruch-Mordo, S., Kiesecker, J.: Global Human Modification. figshare. Dataset. https://doi.org/10.6084/m9.figshare.7283087.v1, 2018.

Klein Goldewijk, K., Van Drecht, G. and Bouwman, A.F.: Mapping contemporary global cropland and grassland distributions on a 5×5 minute resolution. Journal of Land Use Science, 2(3),167-190, 2007.

Klein Goldewijk, K., Beusen, A., Doelman, J. and Stehfest, E.: Anthropogenic land use estimates for the Holocene - HYDE 3.2, Earth Syst. Sci. Data, 9, 927-953. https://doi.org/10.5194/essd-9-927-2017, 2017.

Larson, C.L., Reed, S.E., Merenlender, A.M., Crooks, K.R.: Accessibility drives species exposure to recreation in a fragmented urban reserve network. Landscape and Urban Planning 175:62-71, 2018.

Lehner, B., Liermann, C. R., Revenga, C., Vörösmarty, C., Fekete, B., Crouzet, P., Nilsson, C.: High-resolution mapping of the world's reservoirs and dams for sustainable river-flow management. Frontiers in Ecology and the Environment, 9(9), 494-502, 2011.

Li, X., Zhou, Y.: Urban mapping using DMSP/OLS stable night-time light: a review, International Journal of Remote Sensing, 38:21, 6030-6046, DOI: 10.1080/01431161.2016.1274451, 2017.

~~Larson, C.L., Reed, S.E., Merenlender, A.M., Crooks, K.R.: Accessibility drives species exposure to recreation in a fragmented urban reserve network. Landscape and Urban Planning 175:62-71, 2018.¶~~

Li, W., MacBean, N., Ciais, P., Defourny, P., Lamarche, C., Bontemps, S., Houghton, R. A., and Peng, S.: Gross and net land cover changes in the main plant functional types derived from the annual

ESA CCI land cover maps (1992–2015), Earth Syst. Sci. Data, 10, 219-234, https://doi.org/10.5194/essd-10-219-2018, 2018.
McBride, M. F., Garnett, S. T., Szabo, J. K., Burbidge, A. H., Butchart, S. H., Christidis, L., Burgman, M.A.: Structured elicitation of expert judgments for threatened species assessment: a case study on a continental scale using email. Methods in Ecology and Evolution, 3(5), 906-920, 2012.
Mace, G. M., Barrett, M., Burgess, N. D., Cornell, S. E., Freeman, R., Grooten, M. and Purvis, A., 2018. Aiming higher to bend the curve of biodiversity loss. Nature Sustainability, 1(9), pp.448-451.
Malczewski, J.: GIS and multicriteria decision analysis. John Wiley & Sons, 1999.
Marsh, G. P.: The earth as modified by human action, C. Scribner's Sons, 1885.
Nelson, A.: Travel time to major cities: a global map of accessibility. Report to: Global Environment Monitoring Unit, Joint Research Centre of the European Commission, 2008.
Nelson, A., Weiss, D.J., van Etten, J., Cattaneo, A., McMenomy, T.S., Koo, J.: A suite of global accessibility indicators. *Scientific Data*, 6(1), pp.1-9, 2019.
OpenStreetmap, www.openstreetmap.org. 2019. Accessed April 27, 2019.
Parks, S.A., Carroll, C., Dobrowski, S.Z. and Allred, B.W., 2020. Human land uses reduce climate connectivity across North America. Global Change Biology, 26(5), pp.2944-2955.
Pekel, J. F., Cottam, A., Gorelick, N., Belward, A. S.: High-resolution mapping of global surface water and its long-term changes. Nature, 540(7633), 418, 2016.
Pérez-Hoyos, A., Rembold, F., Kerdiles, H. and Gallego, J.: Comparison of global land cover datasets for cropland monitoring. Remote Sensing, 9(11), p.1118, 2017.
Pesaresi, M., Ehrilch, D., Florczyk, A.J., Freire, S., Julea, A., Kemper, T., Soille, P. and Syrris, V. GHS built-up grid, derived from Landsat, multitemporal (1975, 1990, 2000, 2015). European Commission, Joint Research Centre, JRC Data Catalogue, 2015.
R Core Team: R: A language and environment for statistical computing. R Foundation for Statistical Computing, Vienna, Austria. https://www.R-project.org/, 2019.
Ramankutty, N., Evan, A.T., Monfreda, C. and Foley, J.A.: Farming the planet: 1. Geographic distribution of global agricultural lands in the year 2000. *Global biogeochemical cycles*, *22*(1), 2008.
Riggio, J., Baillie, J.E.M., Brumby, S., Ellis, E., Kennedy, C. M., Oakleaf, J. R., Tait, A., Tepe, T., Theobald, D. M., Venter, O., Watson, J. E. M., Jacobson, A. P.: Global human influence maps reveal clear opportunities in conserving Earth's remaining intact terrestrial ecosystems. Global Change Biology. DOI: 10.1111/gcb.15109, 2020.
Riitters, K.H., Wickham, J.D. and Wade, T.G.: An indicator of forest dynamics using a shifting landscape mosaic. Ecological Indicators, 9(1), pp.107-117, 2009.
Robinson, T. P., Wint, G. W., Conchedda, G., Van Boeckel, T. P., Ercoli, V., Palamara, E., Gilbert, M.: Mapping the global distribution of livestock. PloS one, 9(5), e96084, 2014.
Roszkowska, E.: Rank ordering criteria weighting methods–a comparative overview. OPTIMUM. STUDIA EKONOMICZNE NR 5 (65): 14-33, 2013.
S&P. S&P Global Market Intelligence. Thomson Reuters, New York, United States, 2018.
Salafsky, N., Salzer, D., Stattersfield, A. J., Hilton-Taylor, C., Neugarten, R., Butchart, S. H., Wilkie, D.: A standard lexicon for biodiversity conservation: unified classifications of threats and actions. Conservation Biology, 22(4), 897-911, 2008.

Sanderson, E. W., Jaiteh, M., Levy, M. A., Redford, K. H., Wannebo, A. V., Woolmer, G.: The human footprint and the last of the wild. BioScience, 52(10), 891-904, 2002.
Schultz, M.T.: A critique of EPA's index of watershed indicators. *Journal of Environmental Management*, 62(4), pp.429-442, 2001.
Secretariat of the Convention on Biological Diversity.: Strategic plan for biodiversity 2011–2020 and the Aichi targets, 2010. URL: https://www.cbd.int/sp/targets/default.shtml (Accessed 24 December 2018).
Speirs-Bridge, A., Fidler, F., McBride, M., Flander, L., Cumming, G., Burgman, M.: Reducing overconfidence in the interval judgments of experts. Risk Analysis: An International Journal, 30(3), 512-523, 2010.
Theobald, D.M.: Reducing linear and perimeter measurement errors in raster-based data. Cartography and Geographic Information Science 27(2), 111-116, 2000.
Theobald D.M.: Network and accessibility methods to estimate the human use of ecosystems. In: Proceedings of the 11th AGILE international conference on geographic information science. University of Girona, Spain, 2008.
Theobald, D.M.: Estimating natural landscape changes from 1992 to 2030 in the conterminous US. Landscape Ecology, 25(7), 999-1011, 2010.
Theobald, D.M, Norman, J.B., Newman, P.: Estimating visitor use of protected areas by modeling accessibility: A case study in Rocky Mountain National Park, Colorado. Journal of Conservation Planning, 6:1-20, 2010.
Theobald, D.M.: A general model to quantify ecological integrity for landscape assessments and US application. Landscape Ecology, 28(10), 1859-1874, 2013.
Theobald, D.M.: A general-purpose spatial survey design for collaborative science and monitoring of global environmental change: the global grid. *Remote Sensing*, *8*(10), p.813, 2016.
Theobald, D.M., Kennedy, C., Chen, B., Oakleaf, J., Baruch-Mordo, S., Kiesecker, J.: Data for detailed temporal mapping of global human modification from 1990 to 2017, v4, Dryad, Dataset, https://doi.org/10.5061/dryad.n5tb2rbs1, 2020.
Titeux, N., Henle, K., Mihoub, J. B., Regos, A., Geijzendorffer, I. R., Cramer, W., Verburg, P.H., Brotons, L.: Biodiversity scenarios neglect future land-use changes. Global Change Biology, 22(7), 2505-2515, 2016.
Tobler, W.: Non-isotropic geographic modeling. National Center for Geographic Information and Analysis Technical Report TR-93-1, 1991.
Tulloch, V. J., Tulloch, A. I., Visconti, P., Halpern, B. S., Watson, J. E., Evans, M. C., Giakoumi, S.: Why do we map threats? Linking threat mapping with actions to make better conservation decisions. Frontiers in Ecology and the Environment, 13(2), 91-99, 2015.
UNEP-WCMC and IUCN, Protected Planet: The World Database on Protected Areas (WDPA), February 2019, Cambridge, UK: UNEP-WCMC and IUCN, 2019.
Valenta, R. K., Kemp, D., Owen, J. R., Corder, G. D., Lèbre, É.: Re-thinking complex orebodies: Consequences for the future world supply of copper. Journal of Cleaner Production, 220, 816-826, 2019.
Venter, O., Sanderson, E.W., Magrach, A., Allan, J.R., Beher, J., Jones, K.R., Possingham, H.P., Laurance, W.F., Wood, P., Fekete, B.M., Levy, M.A., Watson, J.E.M.: Global terrestrial Human Footprint maps for 1993 and 2009. Sci. Data 3:160067. DOI: 10.1038/sdata.2016.67, 2016.

Venter, O., Possingham, H.P. and Watson, J.E.: The human footprint represents observable human pressures: Reply to Kennedy et al. *Global Change Biology*, 26(2), pp.330-332., 2019.
Verdone, M., Seidl, A.: Time, space, place, and the Bonn Challenge global forest restoration target. Restoration Ecology, 25, 903–911, 2017.
Vitousek, P. M., Mooney, H. A., Lubchenco, J., Melillo, J. M.: Human domination of Earth's ecosystems. Science, 277(5325), 494-499, 1997.
Waldner, F., Fritz, S., Di Gregorio, A., Plotnikov, D., Bartalev, S., Kussul, N., Löw, F.: A unified cropland layer at 250 m for global agriculture monitoring. Data, 1(1), 3, 2016.
Weiss, D.J., Nelson, A., Gibson, H.S., Temperley, W., Peedell, S., Lieber, A., Hancher, M., Poyart, E., Belchior, S., Fullman, N., Mappin, B.: A global map of travel time to cities to assess inequalities in accessibility in 2015. Nature. 553(7688):333, 2015.
Wickham, J., Stehman, S. V., Gass, L., Dewitz, J. A., Sorenson, D. G., Granneman, B. J., Baer, L. A.: Thematic accuracy assessment of the 2011 national land cover database (NLCD). Remote Sensing of Environment, 191, 328-341, 2017.
WRI. Global Energy Observatory, Google, KTH Royal Institute of Technology in Stockholm, Enipedia, World Resources Institute. Global Power Plant Database. Published on Resource Watch and Google Earth Engine; http://resourcewatch.org, 2019. Accessed 14 April 2019.
Zhang, Q., Pandey, B., Seto, K.C.: A robust method to generate a consistent time series from DMSP/OLS nighttime light data. IEEE Transactions on Geoscience and Remote Sensing 54(10):5821-31, 2016.

Author information

David M. Theobald[1,2], Christina Kennedy[3], Bin Chen[4], James Oakleaf[3], Sharon Baruch-Mordo[3], Joe Kiesecker[3]
[1]Conservation Planning Technologies, Fort Collins, CO 80521, USA
[2]Department of Fish, Wildlife, and Conservation Biology, Colorado State University, Fort Collins, CO 80523, USA
[3]Global Lands Program, The Nature Conservancy, Fort Collins, CO 80524, USA
[4]Department of Land, Air and Water Resources, University of California, Davis, CA 95616, USA

Tables

¶

Table 1. Overview of stressors, datasets, spatial resolution, and years data were available and used in the ~~Human Modification maps~~maps of human modification. Stressor classification levels in parentheses correspond to those within the Direct Threats Classification v2 (Salafsky et al. 2008). ¶

~~**Class**~~¶	~~**Stressor***~~¶	~~**Source**~~¶	~~**Resolution (km^2)**~~¶	~~**Year(s)**~~¶
~~Urban & built-up (1)~~¶	~~Built-up (1.1, 1.2)~~¶	~~Global Human Settlement Layer version R2018A (Pesaresi et al. 2015)~~¶	~~0.0009 - 0.9~~¶	~~1990, 2000, 2010*, 2015~~¶
~~Agriculture (2)~~¶	~~Croplands & pasturelands (2.1)~~¶	~~European Space Agency CCI land cover (Li et al. 2018)~~¶ ~~Unified Cropland Layer (Waldner et al. 2016)~~¶ ~~Global Land Systems v2 (Kehoe et al. 2017)~~¶	~~0.9~~¶ ¶ ~~1~~¶ ¶ ~~1~~¶ ¶	~~1992, 2000, 2010, 2015~~¶ ~~2010~~¶ ¶ ~~2010~~¶ ¶
	~~Grazing (2.3)~~¶	~~Gridded Livestock v3 (Robinson et al. 2014; Gilbert et al. 2018)~~¶	~~10~~¶	~~2010~~¶
~~Energy production & mining (3)~~¶	~~Oil & gas production (3.1)~~¶	~~Nighttime flares from DMSP/OLS and VIIRS (Elvidge et al. 2009; Elvidge et al. 2016)~~¶ ¶	~~0.25 - 1.0~~¶	~~2016~~¶
	~~Mining & quarrying (3.2)~~¶	~~S&P global mining dataset (S&P 2018; Valenta et al. 2019)~~¶	~~~1:10000~~¶	~~1990, 2000, 2010, 2015, 2018~~¶
	~~Renewable (3.3) and non-renewable power (1.2) generation~~¶	~~World Resources Institute Power plants (WRI 2019)~~¶	~~~1:100000~~¶	~~1990, 2000, 2010, 2015, 2018~~¶
~~Transportation & service corridors (4)~~¶	~~Roads (4.1)~~¶	~~OSM highway, minor, and two-track features (OpenStreetMap 2019)~~¶	~~~1:10-25000~~¶	~~2019~~¶
	~~Railways (4.1)~~¶	~~OSM railway features (OpenStreetMap 2019)~~¶	~~~1:10-25000~~¶	~~2019~~¶
	~~Powerlines (4.2)~~¶	~~OSM power line features (OpenStreetMap 2019)~~¶	~~~1:10-25000~~¶	~~2019~~¶

	~~Electrical infrastructure (4.2)~~	~~Nighttime lights from DMSP/OLS and VIIRS (Elvidge et al. 2001; Doll 2008; Elvidge et al. 2013; Zhang et al. 2016)~~	~~0.25 - 1.0~~	~~1992, 2000, 2010, 2015, 2018~~
~~Biological harvesting (5)~~	~~Logging & wood harvesting (5.3)~~	~~Forest loss (Curtis et al. 2018) and forest change (Hansen et al. 2013)~~	~~0.09 - 100~~	~~2000, 2010, 2018~~
~~Human intrusions (6)~~	~~Human intrusions (1.3, 5.1, 5.2, 6.1)~~	~~Human intrusion (Theobald 2008) using accessibility and population from GRUMP v1.01 (CIESIN 2017) and GPW v4 (CIESIN 2018)~~	~~1~~	~~1990*, 2000, 2010, 2015~~
~~Natural system modifications (7)~~	~~Reservoirs (7.2)~~	~~Global Reservoirs and Dams (GRanD v1.3; Lehner et al. 2011); http://globaldamwatch.org/grand/~~	~~~1:25000~~	~~1990, 2000, 2010, 2017~~
~~Pollution (9)~~	~~Air pollution (9.5)~~	~~Emissions Database for Global Atmospheric Research (EDGAR v4.3.2; Crippa et al. 2018) for nitrogen oxides~~	~~~100~~	~~1990, 2000, 2010, 2012~~

Acronyms of source data are bolded in the *Source* column for reference throughout the paper. For each stressor, the years 1990-2015 are used for change analysis, and ~2017 is a compilation of all stressors that represents "current" conditions with the median year of 2017.

Class	**Stressor***	**Source**	**Scale (km^2)**	**Year**				
				1990	**2000**	**2010**	**2015**	**~2017**
Urban & built-up (1)	Built-up (1.1, 1.2)	Global Human Settlement Layer version R2018A (**GHSL**; Pesaresi et al. 2015)	0.0009 - 0.9	1990	2000	2010*	2015	2015
Agriculture (2)	Croplands & pasturelands (2.1)	European Space Agency Climate Change Initiative land cover (**ESA CCI**; Li et al. 2018) Unified Cropland Layer (**UCL**; Waldner et al. 2016) Global Land Systems v2 (**GLS**; Kehoe et al. 2017)	0.9 1 1	1992	2000	2010 2010 2010	2015	2015 2010 2010
	Grazing (2.3)	Gridded Livestock of the World v3 (**GLW**; Robinson et al. 2014; Gilbert et al. 2018a, Gilbert et al. 2018b)	10			2010		2010

Energy production & mining (3)	Oil & gas production (3.1)	Nighttime flares from Defense Meteorological Program/Operational Line-scan System (**DMSP/OLS**, Elvidge et al. 2009) and Visible Infrared Imaging Radiometer Suite (**VIIRS**, Elvidge et al. 2016)	0.25 - 1.0					2016
	Mining & quarrying (3.2)	S&P global mining dataset (S&P 2018; Valenta et al. 2019)	~1:100 00	1990,	2000	2010	2015	2018
	Renewable (3.3) & non-renewab le power (1.2) generation	World Resources Institute Power plants (**WRI**; WRI 2019)	~1:100 000	1990	2000	2010	2015	2018
Transporta tion & service corridors (4)	Roads (4.1)	OpenStreetMap highway, minor, and two-track features (**OSM**; OpenStreetMap 2019)	~1:10-2 5000	**			**	2019
	Railways (4.1)	OSM railway features (OpenStreetMap 2019)	~1:10-2 5000					2019
	Powerlines (4.2)	OSM power line features (OpenStreetMap 2019)	~1:10-2 5000					2019
	Electrical infrastructur e (4.2)	Nighttime lights from **DMSP/OLS** and **VIIRS** (Elvidge et al. 2001; Doll 2008; Elvidge et al. 2013; Zhang et al. 2016)	0.25 - 1.0	1992	2000	2010	2015	2018
Biological harvesting (5)	Logging & wood harvesting (5.3)	Forest loss (Curtis et al. 2018) and forest change (Hansen et al. 2013)	0.09 - 100	2000	2000	2010	2015	2018
Human intrusions (6)	Human intrusions (1.3, 5.1, 5.2, 6.1)	Human intrusion (Theobald 2008, **HUE**) using accessibility and population from Global Rural-Urban Mapping Project v1.01 (**GRUMP**; CIESIN 2017) and Gridded	1	1990*	2000	2010	2015	2015

		Population of the World v4 (**GPW;** CIESIN 2018)						
Natural system modifications (7)	Reservoirs (7.2)	Global Reservoirs and Dams (**GRanD** v1.3; Lehner et al. 2011)	~1:250 00	1990	2000	2010	2015	2017
Pollution (9)	Air pollution (9.5)	Emissions Database for Global Atmospheric Research (**EDGAR** v4.3.2; Crippa et al. 2018) for NO_x	~100	1990	2000	2010	2012	2012

*Based on interpolation.¶

**Used major roads (i.e. highways) for 2019.

Table 2. Estimates of the intensity value for each stressor. "Best" estimates were determined from Brown and Vivas (2005)[1], Theobald (2013)[2], Kennedy et al. (2019a)[3], or expert judgement[4], and are bracketed by a minimum and maximum range, following the lowest-highest-best estimate elicitation procedure to reduce bias (McBride *et al.*, 2012). Results presented here use the best estimate, while minimum and maximum estimates are used to specify the range of possible randomized intensity values in the uncertainty analysis.

Class	Stressor	Minimum	Best	Maximum
Urban & built-up	Built-up areas[3,4]	0.69	0.85	1.00
Agriculture	Cropland/pasture[3] - Minimal[4] - Light[4] - Intense[1,4]	 0.29 0.35 0.60	 0.34 0.45 0.65	 0.39 0.55 0.70
	Livestock grazing[1]	0.20	0.28	0.37
Energy production & mining	Oil & gas production[1,3]	0.70	0.85	1.00
	Mining[3]	0.83	0.91	1.00
	Power generation[1] (non-renewable)	0.70	0.85	1.00
	Power generation (renewable)[1]	0.70	0.80	0.90
Transportation & service corridors*	Major roads[1]	0.78 (20)	0.80 (30)	0.83 (40)
	Minor roads[1]	0.39 (15)	0.44 (20)	0.50 (25)
	Two-track roads[1]	0.10 (3)	0.15 (5)	0.20 (10)
	Railways[1]	0.78 (15)	0.80 (20)	0.83 (25)
	Powerlines[2]	0.10	0.15	0.20
	Electrical infrastructure (night-time lights)[3]	0.20	0.35	0.50
Biological harvesting	Logging & wood harvesting[1,4]** - Commodity-driven[1,4] - Shifting agriculture[1,4] - Forestry[1,4]	 0.60 0.10 0.10	 0.65 0.20 0.20	 0.07 0.30 0.30

Human intrusion	Human intrusion[3,4]	0.20	0.35	0.50
Natural systems modification	Reservoirs[4]	0.60	0.65	0.70
Pollution	Air pollution[4,] ****	0.05	0.10	0.20

*Assumed width of roads and railways (meters) provided in parentheses. *Use* of roads is incorporated into estimates of human "intrusion".

**Causes of forest loss due to wildfire was not included because of the challenges in understanding human-causation/suppression, especially over a global extent. Also, cause of loss due to urbanization was not included in this stressor because it is incorporated directly in the built-up stressor.

***Minimum value is half of best, maximum is twice of best.

Table 3. Probability of a land cover type being classified as cropland or pasture, calculated using the producer's accuracy, which is how often features on the ground are classified, or the probability that a certain pixel is classified as a given land cover class. Probabilities of being cropland or pasture cover type (C_{cp}) are adjusted based on patch size (A) for patches with A < 1 km^2, where $p(C_{cp}) = C_{cp} * A_{cp}^{\ 2}$.

Value	Name	Crop/ pastureland weight	Proability crop/pastureland
10	Cropland, rainfed	1	0.887
20	Cropland, irrigated	1	0.893
30	Mosaic cropland (>50%)	0.5	0.387
40	Mosaic cropland (>50%)	0.25	0.366
50	Tree (>15%), broadleaved, evergreen	0	0.038
60	Tree (>15%), broadleaved, deciduous	0	0.070
70	Tree (>15%), needleleaved, evergreen	0	0.016
80	Tree (>15%, neeleeaved, deciduous	0	0.000
90	Tree, mixed leaf type	0	0.000
100	Mosaic tree/shrub (>50%)	0	0.345
110	Mosaic herbaceous (>50%)	0	0.091
120	Shrubland	0	0.104
130	Grassland	0	0.176
140	Lichens and mosses	0	0.000
150	Sparse vegetation (<15%)	0	0.032
160	Tree, flooded	0	0.043
170	Tree, flooded saline	0	0.000
180	Shrub/herbaceous flooded	0	0.000
190	Urban areas	0	0.120
200	Bare	0	0.011
210	Water	0	0.018
220	Permanent snow & ice	0	0.000

Table 4. Summary of estimates ~~(H)~~ of the degree of human modification (*H*) and the mean annualized difference between 5- or 10-yr increments for which change over time can be calculated (1990, 2000, 2010, and 2015), and *H* values for the contemporary dataset (~2017, all stressors). Mean annualized mean difference is calculated as the mean value across the continents of the difference in *H* values divided by the number of years (e.g., $H_{mad}=[H_{2015}-H_{1990}]/25$).

	Mean H				**Mean annualized difference**				**~2017**		
Continent	**1990**	**2000**	**2010**	**2015**	**1990-2000**	**2000-2010**	**2010-2015**	**1990-2015**	**Med-ian**	**Mean**	**Std. Dev.**
Africa	0.0457	0.0489	0.0515	0.0530	0.00032	0.00026	0.00030	0.00029	0.0056	0.1073	0.1730
Asia	0.0856	0.0915	0.0988	0.1025	0.00059	0.00073	0.00075	0.00067	0.0056	0.1542	0.2286
Australia	0.0313	0.0324	0.0334	0.0341	0.00011	0.00011	0.00013	0.00011	0.0006	0.0495	0.1250
Europe	0.1145	0.1187	0.1206	0.1226	0.00042	0.00019	0.00041	0.00033	0.0136	0.1533	0.2279
No. America	0.0408	0.0419	0.0461	0.0463	0.00011	0.00042	0.00005	0.00022	0.1309	0.1680	0.1681
Oceania	0.0431	0.0475	0.0580	0.0662	0.00044	0.00105	0.00164	0.00093	0.0527	0.1592	0.1856
So. America	0.2378	0.2398	0.2434	0.2442	0.00020	0.00036	0.00015	0.00026	0.2324	0.2868	0.2717
Global	0.0822	0.0864	0.0915	0.0946	0.00042	0.00051	0.00062	0.00049	0.0096	0.1461	0.2146

Table 5. A comparison of the mean annualized difference of human modification values for changes from 1990 to 2015 (~~HM~~H, 1990-2015), human footprint (HF, 1993-2009; Venter et al. 2016), and the temporal human pressure index (THPI, 1995-2010, Geldmann et al. 2019). Mean annualized mean difference is calculated as the mean value of the difference in *H* values divided by the number of years (e.g., $H_{mad}=[H_{2015}-H_{1990}]/25$)~~.~~, for each continent. Note that Oceania extends below Papau New Guinea (excluding the country of Australia).

Continent	HM	HF	THPI
Africa	~~0.00029~~0.0003	~~0.00069~~0.0007	~~0.00106~~0.0011
Asia	~~0.00068~~0.0007	~~0.00085~~0.0008	~~0.00123~~0.0012
Australia	~~0.00011~~0.0001	~~0.00018~~0.0002	~~0.00012~~0.0001
Europe	~~0.00033~~0.0003	-~~0.00023~~0.0002	~~0.00024~~0.0002
North America	~~0.00022~~0.0002	~~0.00271~~0.0027	-~~0.00014~~0.0001
Oceania	~~0.00093~~0.0009	~~0.00113~~0.0011	~~0.00072~~0.0007
South America	~~0.00025~~0.0003	~~-0.00004~~0.0000	~~0.00024~~0.0002
Global	~~0.00050~~0.0005	~~0.00056~~0.0006	~~0.00081~~0.0008

Table 6. A summary of the data, methods, and results comparing the degree of human modification (HM; this paper); degree of human modification 1 km (HM1k; Kennedy et al. 2019a, 2019b, 2019c); human footprint (HF; Sanderson et al. 2002; Venter et al. 2016); and temporal human pressure index (THPI; Geldmann et al. 2019). Also see discussion of comparison in Kennedy et al. (2019b, 2019c), Venter et al. (2019), and Riggio et al. (2020). Data source acronyms are provided in Table 1.

Factor	HM	HM1k	HF	THPI
Conceptual framework	Direct Threats Classification v2 (Salafsky et al. 2008) Intensity values based on Land Development Index (LDI; Brown and Vivas 2005)	Direct Threats Classification v2 (Salafsky et al. 2008) LDI	Sanderson et al. (2002)	Geldmann et al. (2014)
Stressor: Urban and built-up	Urban and built-up (GHSL; 0.03-0.3 km; 1990-2015)	Urban and built-up (GHSL; 0.03-0.3 km; 2015) Population density (GPW v4 2015, 1 km)	Night-time lights (DMSP/OLS >20; 1 km; 1994-2012) Population density CIESIN v3; 4 km; 1990, 2010)	Change in population density (GPW v3 1995, 2010, 1 km)
Stressor: Agriculture	Cropland & pastureland for 1990, 2015 (ESA CCI; 300 m) and Cropland intensity (GLS, 1 km) Unified Cropland Layer (UCL, 1 km) Grazing (GLW, 10 km, 1 < livestock units/km² < 1000)	Unified Cropland Layer (UCL, 1 km) Grazing (GLW v2, 1 km, livestock units/km² < 1000)	Cropland (UMD for 1990 and GlobCover for 2009); Pastureland (2000), 10 km	Cropland area (HYDE, 10 km)
Stressor: Energy production & mining	Oil & gas production (Gas flares DMSP/OLS and VIIRS) Renewable and non-renewable power plants (WRI) Large mining operations (S&P)	Oil & gas wells, wind turbines, mines (OSM, 2016, VMAP0-2000)	N/A	N/A
Stressor: Transportation & service corridors	Road (highway, minor, two-track; OSM, 2019) Railways (OSM, 2019) Powerlines (OSM, 2019) Electrical power infrastructure (harmonized DMSP/ VIIRS, 1992-2018)	Road (highway, minor, two-track, OSM, 2016, gROADS-2000) Railways (OSM, 2016, VMAP0-2000), Powerlines (OSM 2016) Electric infrastructure (night-time lights DMSP-OLS-2013)	Roads (gROADS, 1980-2000); Railways (VMAP-2000) Electric infrastructure	Nightlights (DMSP/OLS nightlights >20; 1 km; 1994-2012)
Stressor: Biological harvesting	Forest loss (Hansen, Curtis; 0.03-1 km, 2000-2017)	N/A	N/A	N/A
Stressor: Human intrusions	Human intrusion (HUE, 1990-2015, 1 km)	N/A	N/A	N/A
Stressor:	Reservoirs (GRanD, 1990-2017,	N/A	N/A	N/A

Natural system modifications	0.03 km)			
Stressor: Pollution	Nitrous oxide pollution (EDGAR, 1990-2012, 100 km)	N/A	N/A	N/A
Metric	Degree of human modification (H, 0-1.0 continuous value)	Degree of human modification (H, 0-1.0 continuous value)	Scaled 0-10, 0-4, summed to 50, ordinal value	N/A
Combine factors	Increasive to 1.0 using fuzzy sum	Increasive to 1.0 using fuzzy sum	Additive, max-normalized	Equal-weight, additive normalized
Uncertainty or sensitivity analysis	Calculates per-pixel variance due to estimates of intensity values, randomized (n=50)	Calculates per-pixel variance due to estimates of intensity values, randomized (n=100)	Sensitify of static v. dynamic pasture data	N/A
Validation	Tested using independent validation dataset that included ~10,000 subplots within ~1,000 1 km^2 sample plots	Tested using independent validation dataset that included ~10,000 subplots within ~1,000 1 km^2 sample plots	Tested using independent validation dataset in 3,460 1 km^2 sample plots	N/A

Table ~~6~~7. Summary of results by biome, comparing trends using the mean annualized difference for the human modification (~~HM_{mad}~~H_{mad}), human footprint (HF_{mad}, Venter et al. 2016), and the mean temporal human pressure index ($THPI_{mad}$, Geldmann et al. 2019) score. Also provided are estimates of the proportion of terrestrial lands modified as estimated ~~by HM, human modification~~ from Kennedy et al. (~~HM1k~~H1k; 2019), and HF (score was max-normalized to rescale to 0-1). The THPI dataset ~~only characterizes~~characterizes only change and so estimates of the proportion of lands modified in 2010 could not be provided. Mean annualized mean difference is calculated as the mean value across the continents and globally of the difference in H values divided by the number of years.

Biome name	~~HM_{mad}~~HM (1990-2015)	~~HF_{mad}~~HF (1993-2009)	~~$THPI_{mad}$~~THPI* (1995-2010)	HM (~2017)	~~HM1k~~HM** (~2016)	HF (2009)
Boreal Forests/Taiga	~~0.000004~~ 0.00000	~~-0.000014~~ 0.00001	~~0.000001~~ 0.00000	0.0213	0.0374	0.0288
Deserts & Xeric Shrublands	~~0.000010~~0.00001	~~0.000028~~ 0.00003	~~0.000032~~ 0.00003	0.0571	0.1059	0.0820
Flooded Grasslands & Savannas	~~0.000022~~0.00002	~~0.000023~~0.00002	~~0.000152~~0.00015	0.2024	0.2480	0.1423
Mangroves	~~0.000050~~ 0.00005	~~0.000047~~ 0.00005	~~0.000021~~0.00002	0.2165	0.3051	0.1972
Mediterranean Forests, Woodlands & Scrub	~~0.000033~~ 0.00003	~~0.000078~~ 0.00008	~~0.000120~~0.00012	0.2903	0.3373	0.2162
Montane Grasslands & Shrublands	~~0.000013~~0.00001	~~0.000059~~ 0.00006	~~0.000057~~ 0.00006	0.0894	0.1634	0.1076
Temperate Broadleaf & Mixed Forests	~~0.000023~~0.00002	~~0.000027~~0.00003	~~0.000022~~ 0.00002	0.3744	0.3968	0.2485
Temperate Conifer Forests	~~0.000016~~0.00002	~~0.000011~~0.00001	~~0.000057~~ 0.00006	0.1072	0.1561	0.0992
Temperate Grasslands, Savannas & Shrublands	~~0.000015~~0.00002	~~0.000006~~ 0.00001	~~0.000092~~ 0.00009	0.2374	0.2943	0.1668
Tropical & Subtropical Coniferous Forests	~~0.000032~~0.00003	~~0.000005~~ 0.00000	~~0.000247~~ 0.00025	0.2052	0.2606	0.1568
Tropical & Subtropical Dry Broadleaf Forests	~~0.000046~~ 0.00005	~~0.000118~~0.00012	~~0.000056~~ 0.00006	0.3317	0.4242	0.2265
Tropical & Subtropical Grasslands, Savannas & Shrublands	~~0.000020~~ 0.00002	~~0.000057~~ 0.00006	~~0.000084~~ 0.00008	0.1476	0.2120	0.1207
Tropical & Subtropical Moist Broadleaf Forests	~~0.000047~~ 0.00005	~~0.000074~~ 0.00007	~~0.000092~~ 0.00009	0.1862	0.2310	0.1390
Tundra	~~0.000001~~0	~~0.000001~~0	~~-0.000001~~	0.0023	0.0001	0.0066

	.00000	.00000	0.00000			

¶

¶

¶

¶

Figure captions

Figure 1. A comparison of the recent trends in human activities by ecoregion using the mean annualized difference estimated by: (a) human modification (*H*, from 1990-2015); (b) human footprint (for 1993-2009, Venter et al. 2016); and (c) temporal human pressure index (for ~1995-2010, Geldmann et al. 2019). Note: interactive maps are available ~~here~~at: https://davidtheobald8.users.earthengine.app/view/global-human-modification-change.

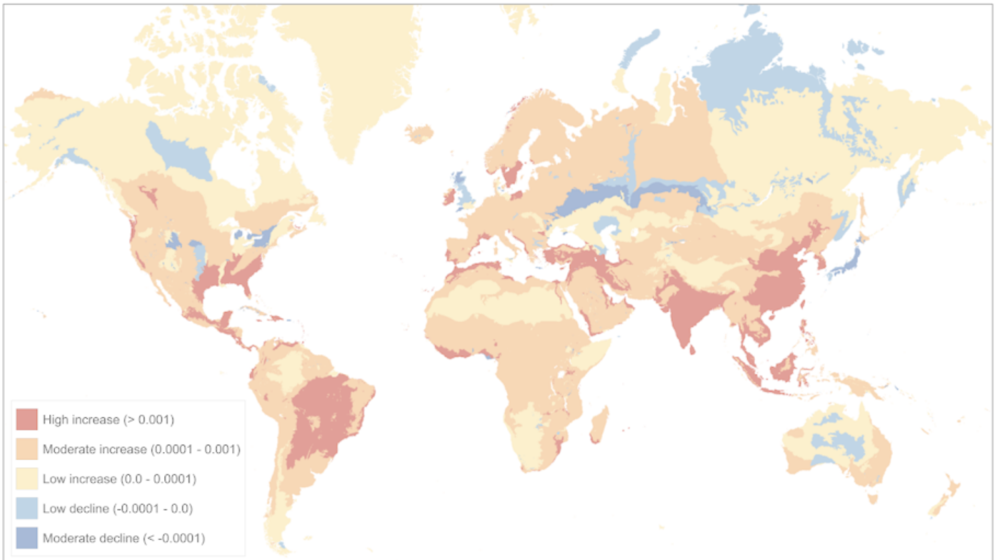
High increase (> 0.001)
Moderate increase (0.0001 - 0.001)
Low increase (0.0 - 0.0001)
Low decline (-0.0001 - 0.0)
Moderate decline (< -0.0001)

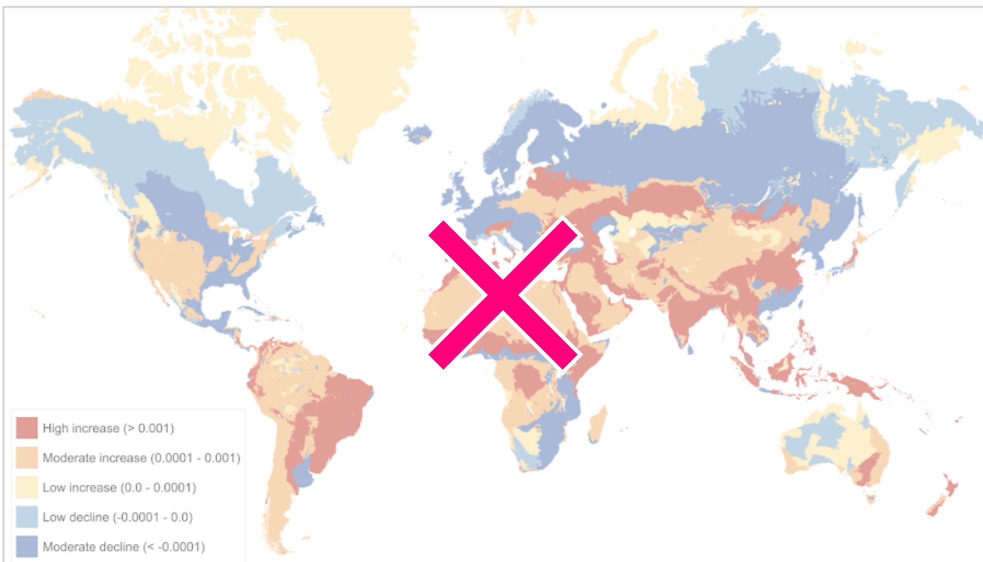
High increase (> 0.001)
Moderate increase (0.0001 - 0.001)
Low increase (0.0 - 0.0001)
Low decline (-0.0001 - 0.0)
Moderate decline (< -0.0001)

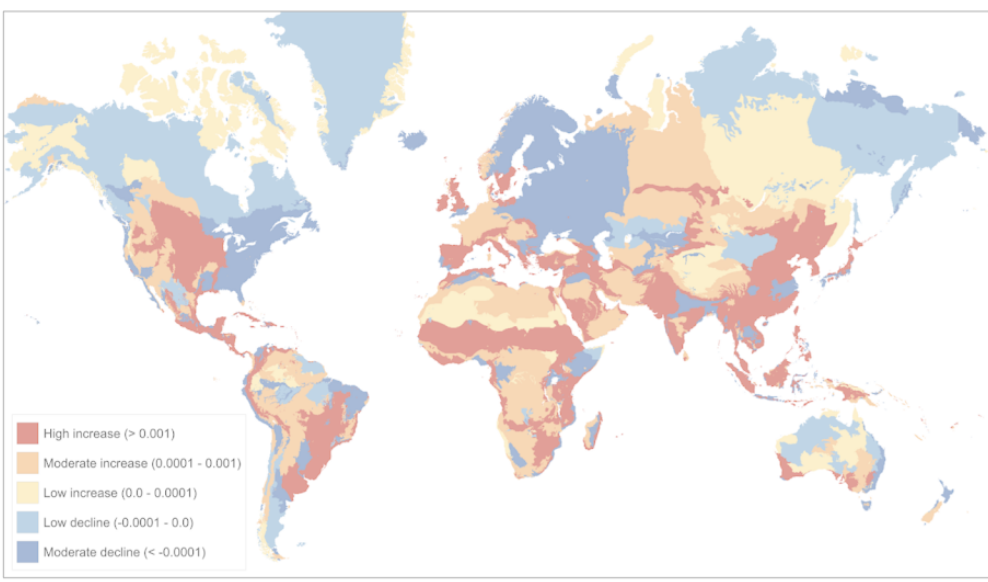
High increase (> 0.001)
Moderate increase (0.0001 - 0.001)
Low increase (0.0 - 0.0001)
Low decline (-0.0001 - 0.0)
Moderate decline (< -0.0001)

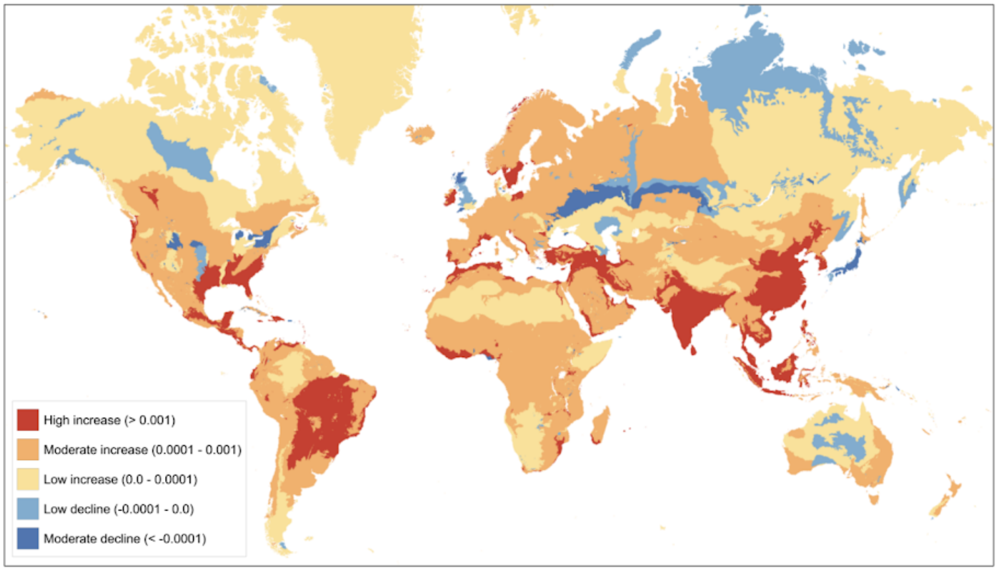
High increase (> 0.001)
Moderate increase (0.0001 - 0.001)
Low increase (0.0 - 0.0001)
Low decline (-0.0001 - 0.0)
Moderate decline (< -0.0001)

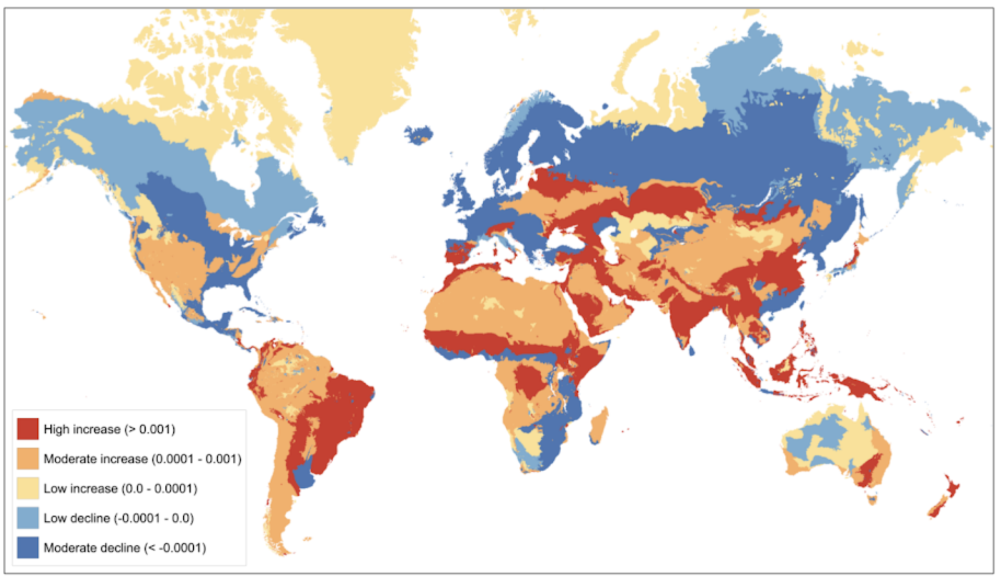
High increase (> 0.001)
Moderate increase (0.0001 - 0.001)
Low increase (0.0 - 0.0001)
Low decline (-0.0001 - 0.0)
Moderate decline (< -0.0001)

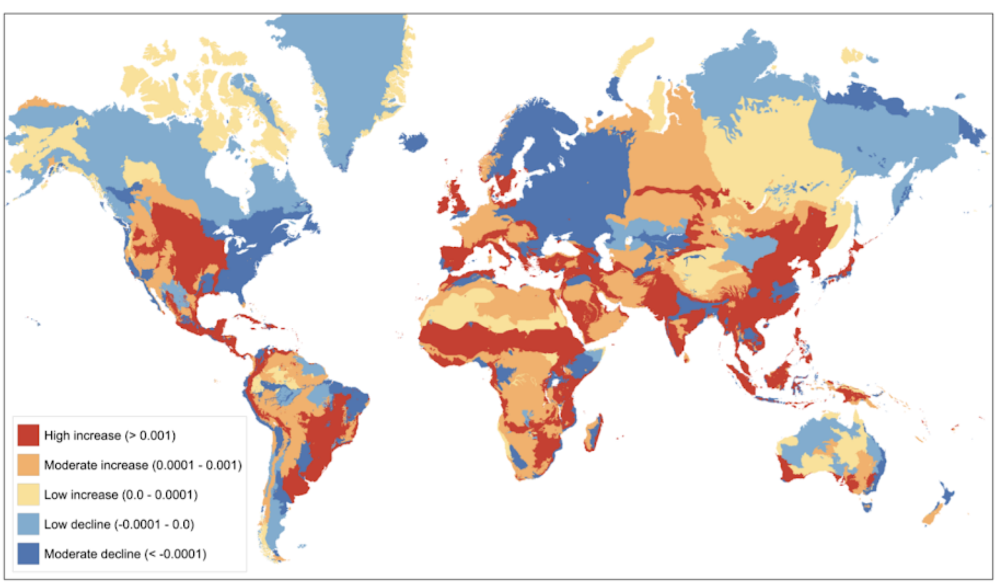
High increase (> 0.001)
Moderate increase (0.0001 - 0.001)
Low increase (0.0 - 0.0001)
Low decline (-0.0001 - 0.0)
Moderate decline (< -0.0001)

Figure 2. Graphs of the ratio of natural lands loss (2015:1990) and contemporary (~2017) degree of human modification (denoted as HM) for each of the 14 biomes and its ecoregions, globally. Note that ecoregions with change ratios ≥3.0 are placed on the maximum x-axis value (3.0).

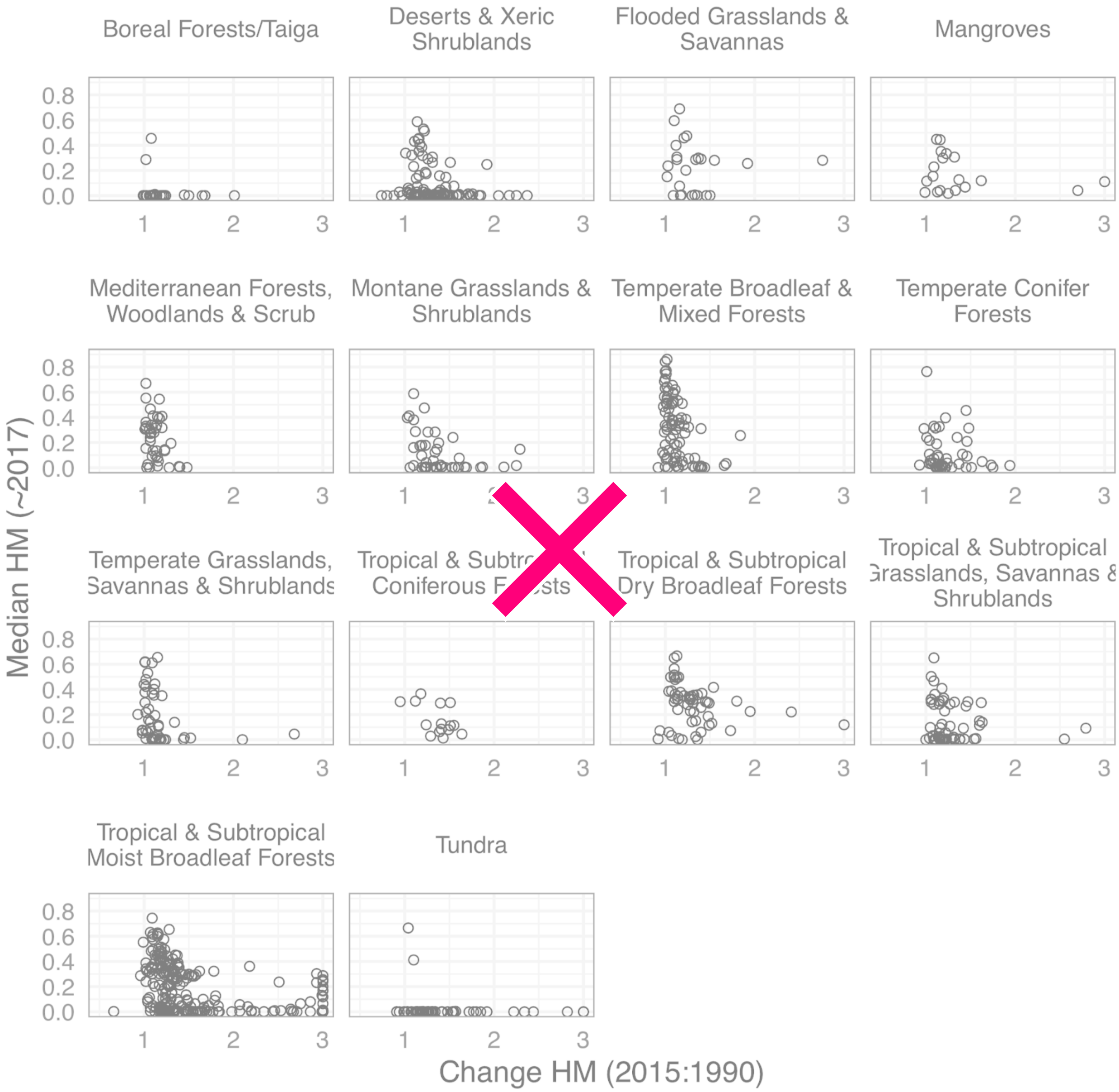
Boreal Forests/Taiga
Deserts & Xeric Shrublands
Flooded Grasslands & Savannas
Mangroves
Mediterranean Forests, Woodlands & Scrub
Montane Grasslands & Shrublands
Temperate Broadleaf & Mixed Forests
Temperate Conifer Forests
Temperate Grasslands, Savannas & Shrublands
Tropical & Subtropical Coniferous Forests
Tropical & Subtropical Dry Broadleaf Forests
Tropical & Subtropical Grasslands, Savannas & Shrublands
Tropical & Subtropical Moist Broadleaf Forests
Tundra
Median HM (~2017)
Change HM (2015:1990)

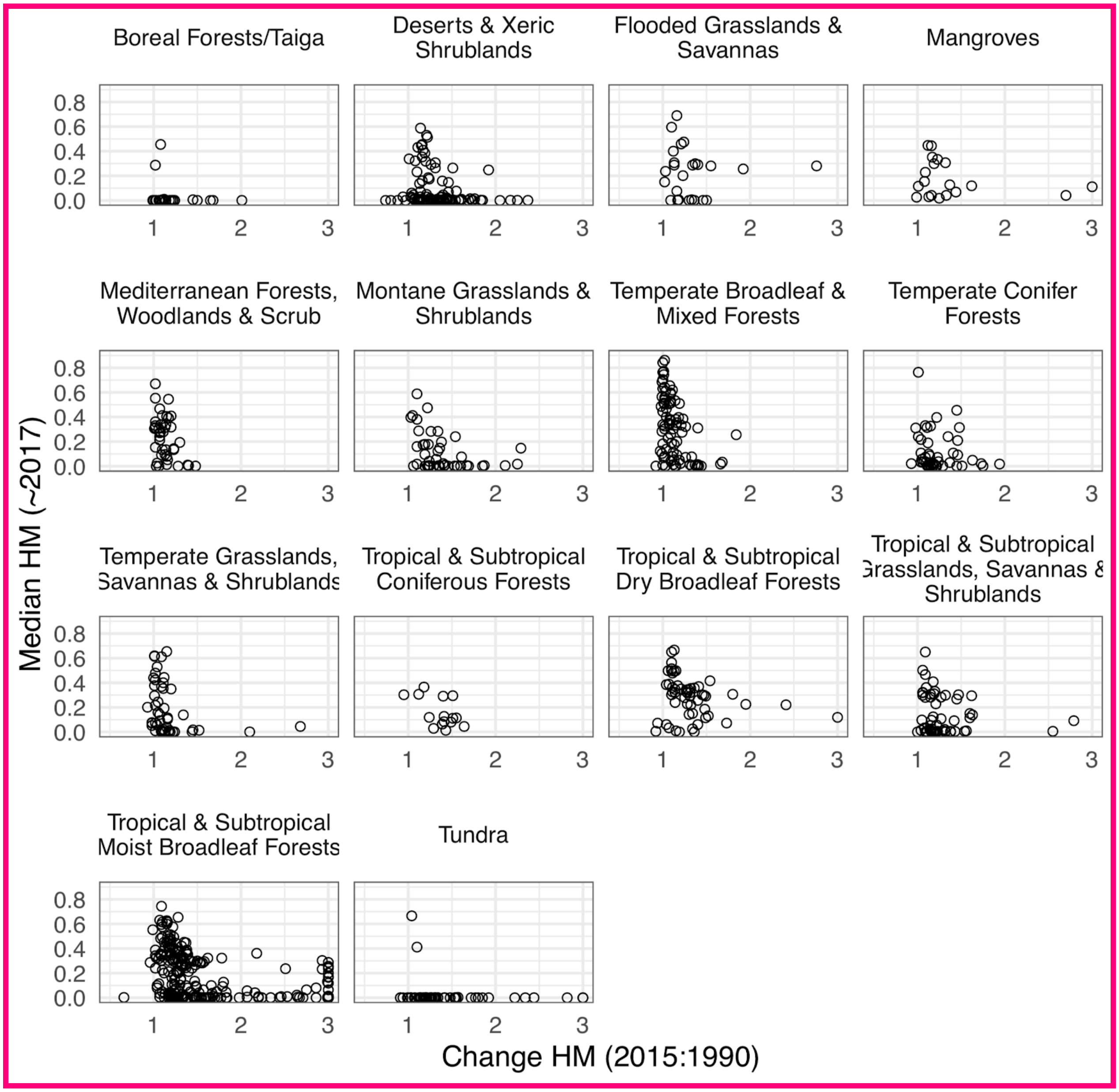
Boreal Forests/Taiga
Deserts & Xeric Shrublands
Flooded Grasslands & Savannas
Mangroves
Mediterranean Forests, Woodlands & Scrub
Montane Grasslands & Shrublands
Temperate Broadleaf & Mixed Forests
Temperate Conifer Forests
Temperate Grasslands, Savannas & Shrublands
Tropical & Subtropical Coniferous Forests
Tropical & Subtropical Dry Broadleaf Forests
Tropical & Subtropical Grasslands, Savannas & Shrublands
Tropical & Subtropical Moist Broadleaf Forests
Tundra
Median HM (~2017)
Change HM (2015:1990)
0.0
0.2
0.4
0.6
0.8
1
2
3

Figure 3. The degree of human modification for circa ~2017: (a) globally; (b) central America; (c) Europe, and (d) Oceania. Note: interactive maps are available ~~here~~at: https://davidtheobald8.users.earthengine.app/view/global-human-modification-change.

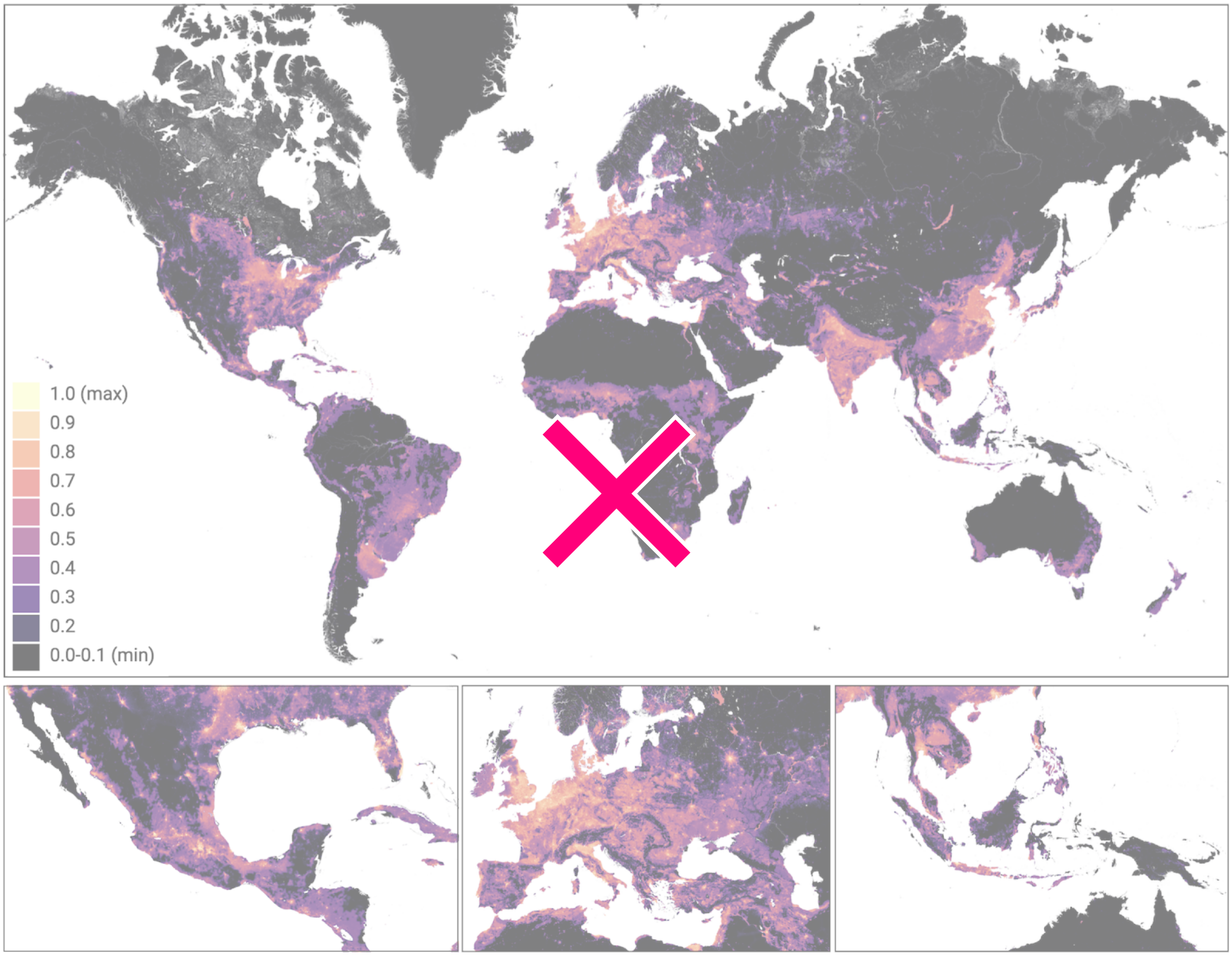
1.0 (max)
0.9
0.8
0.7
0.6
0.5
0.4
0.3
0.2
0.0-0.1 (min)

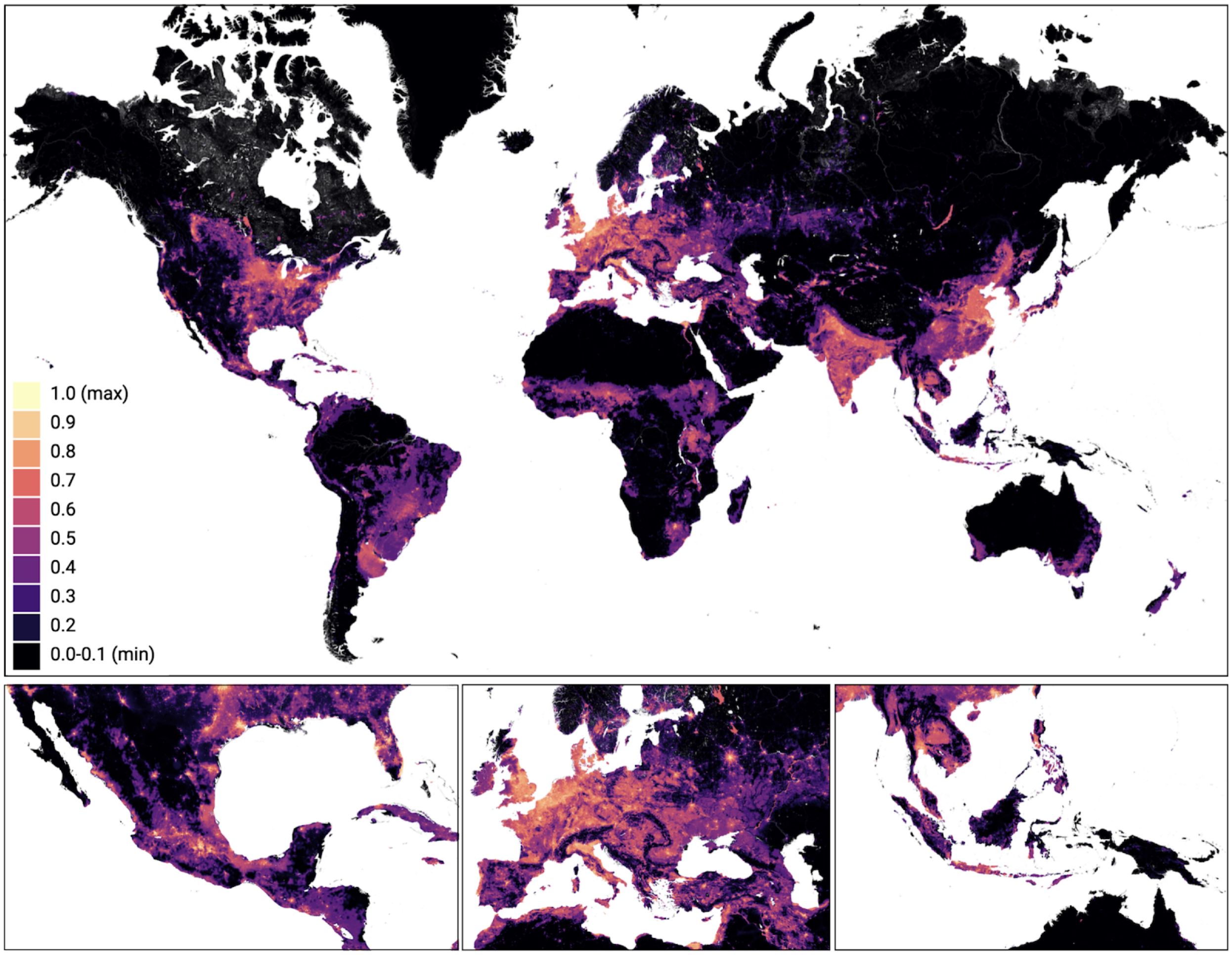
1.0 (max)
0.9
0.8
0.7
0.6
0.5
0.4
0.3
0.2
0.0-0.1 (min)

¶

¶

¶

¶

¶

¶

Figure 4. A map of the uncertainty as a result of randomizing the intensity factors when calculating the degree of human modification for 2017, showing the per-pixel standard deviation of 50 randomized maps. The highest levels of uncertainty tend to be in more highly developed landscapes (minimum=0.0, median=0.0, mean=0.009, standard deviation= 0.014, maximum=0.186).